Fractal Growth Phenomena

Tamás Vicsek

Institute for Technical Physics
Budapest, Hungary

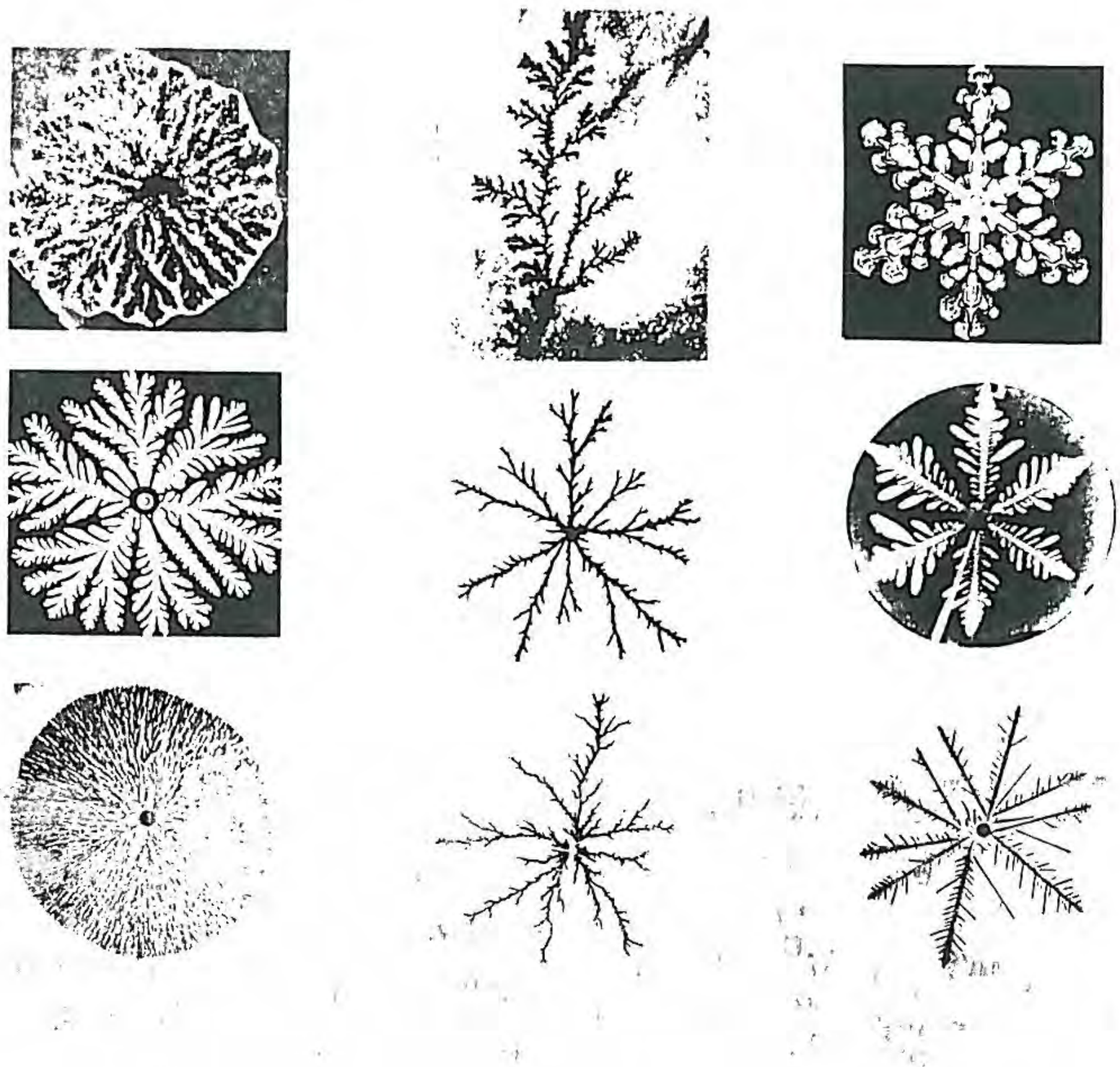

WORLD SCIENTIFIC
Singapore

$D = A \cdot b^{\alpha}$

/

Scaling, $C(r) \sim A r^{\alpha}$ $r \to br$ $C(br) \sim D r^{\alpha}$
new - analitikus, kritikus viselkedés, kritikus pont
universális kritikus exponenser

PART II.

CLUSTER GROWTH MODELS

Chapter 6.

DIFFUSION-LIMITED GROWTH

Many of the growth processes in nature are governed by the spatial distribution of a field-like quantity which is inherently *non-local*, i.e., the value of this quantity at a given point in space is influenced by distant points of the system, in addition to its immediate neighbourhood. For example, such behaviour is exhibited by the distribution of temperature during solidification, the probability of finding a diffusing particle or cluster at a given point, and electric potential around a charged conductor.

The spatial dependence of these quantities in various approximations satisfies the *Laplace equation with moving boundary conditions.* Since the concentration of diffusing particles is also described by the Laplace equation, the above mentioned class of processes is commonly called diffusion-limited growth. Diffusion-limited motion of interfaces typically leads to very complex, branching fractal objects, because of the unstable nature of growth. Thus, as a result of a self-organizing mechanism governed by the Laplace equation, structures with a rich geometry can emerge from the originally homogeneous, structureless medium. This far-from equilibrium phenomenon can be studied by approaches based on aggregation.

It is the non-local character of the probablity distribution which plays an essential role in aggregation phenomena, where single particles, or clusters of particles are added to a growing aggregate. The main assumption of

the related cluster models is that the particles stick together irreversibly, a condition which is satisfied in a wide variety of growth processes.

6.1. DIFFUSION-LIMITED AGGREGATION (DLA)

Consider an electrolite containing positive metallic ions in a small concentration, and a negative electrode. Whenever a randomly diffusing ion hits the electrode or the already deposited metal on its surface, it stops moving (sticks to the surface rigidly) because of the electrostatic attraction. This experiment results in a complicated, tree-like deposit with scale-invariant structure.

The model called *diffusion-limited aggregation* (DLA) was introduced by Witten and Sander (1981) to simulate in a computer phenomena related to the above mentioned process. The rules of the model are simple: One puts a seed particle at the origin of a lattice. Another particle is launched far from the origin and is allowed to walk at random (diffuse) until it arrives at a site adjacent to the seed particle. Then it is stopped, and another particle is launched which stops when adjacent to the two occupied sites, and so forth. In this way large clusters can be generated whose structure is expected to be characteristic for objects grown under diffusion-limited conditions. Indeed, the experiments discussed in Chapter 10. support this expectation.

Fig. 6.1 shows a typical DLA cluster of 3000 particles. It demonstrates that these objects i) have a randomly branching, open structure, ii) look stochastically self-similar, and iii) this special geometry is likely to be due to the effects of screening. By stochastic self-similarity here we mean the following: shrinking a large branch and omitting the finest details one obtains a structure which has the same appearance as a smaller branch. In the case of DLA screening is manifested through the fact that the tips of most advanced branches capture the incoming diffusing particles most effectively. Thus, small fluctuations are enhanced, and this instability together with the randomness inherent in the model leads to a complex behaviour (Witten and Sander 1981, 1983).

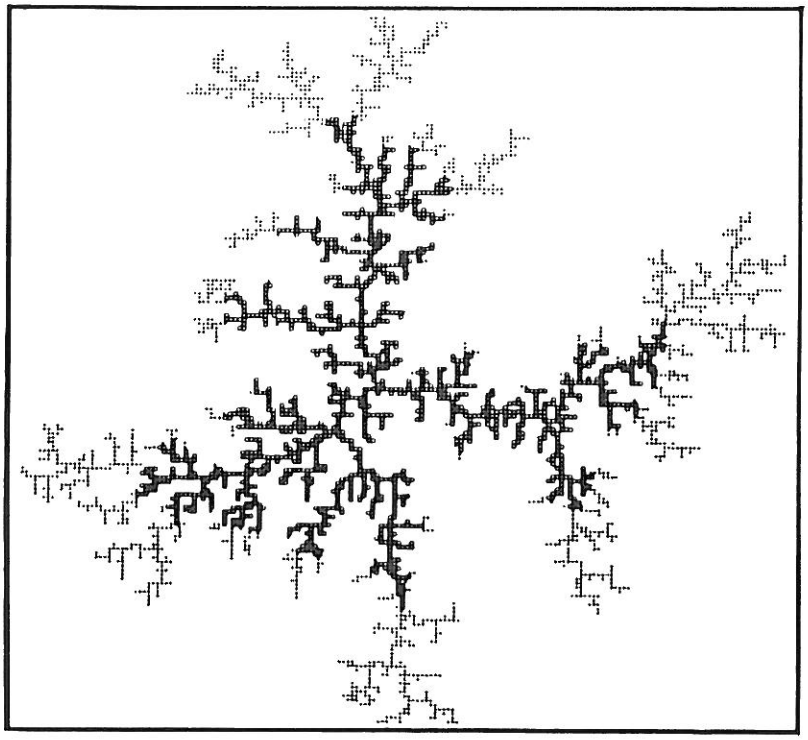

Figure 6.1. A relatively small DLA cluster consisting of 3000 particles. To demonstrate the screening effect the first 1500 particles attached to the aggregate are open circles, while the rest are dots (Witten and Sander 1983).

In the actual simulations the rules are changed in such a way that the resulting process is equivalent to the original version, but it can be realized much more efficiently in a computer. For example, the particles can be launched from a circle having a radius which is only a little larger than the distance of the furthermost particle (belonging to the cluster) from the origin. This can be done because a particle released very far from the cluster arrives at the points of a circle centred at the origin with the same probability. However, as soon as a diffusing particle enters this circle, its trajectory has to be followed until it either sticks to the cluster or diffuses far away. Only in the latter case can it be put back onto the launching circle again. There are additional relevant improvements in the algorithm (Meakin 1985) which are described in Appendix A.

6.1.1. Fractal dimension

The fractal dimension of diffusion-limited aggregates can be estimated by methods described in Section 4.2. As discussed, a possible way to determine the fractal dimension defined by the expression

$$N(R) \sim R^D \tag{6.1}$$

is to calculate the density-density correlation function $c(r)$ (2.14). Fig. 6.2 shows $c(r)$ obtained for DLA clusters grown on a square lattice as a function of the distance r between the particles (Meakin 1983a). The slope of the straight line fitted to the data on this double logarithmic plot indicates that the density correlations within the clusters decay according to a power law

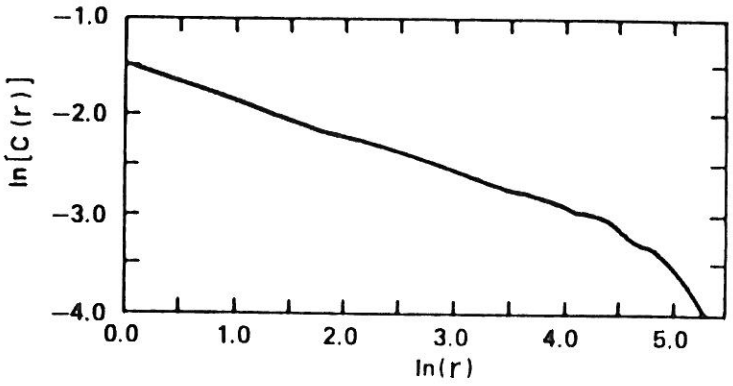

Figure 6.2. Double logarithmic plot of the density-density correlation function $c(r)$ (2.14) for a DLA cluster of 11260 particles generated on the square lattice (Meakin 1983a).

$$c(r) \sim r^{-\alpha} \tag{6.2}$$

with $\alpha \simeq 0.3$ in $d = 2$. An alternative method is to determine the radius of gyration of the clusters $R_g(N)$ (4.12) as a function of the number of particles N. Plots of this kind demonstrate that (Meakin 1983a)

$$R_g(N) \sim N^{\nu}, \tag{6.3}$$

where $\nu = 1/D \simeq 0.585$. These results are in good agreement with the expression (2.18) (Witten and Sander 1981) for the fractal dimension $D = d - \alpha \simeq 1.7$. Therefore, the mass (number of particles) within a region of radius R of a diffusion-limited aggregate scales as $N \sim R^D$ which is equivalent to expression (2.4).

Dependence of the fractal dimension of DLA clusters on the embedding dimension and the sticking probability was extensively studied by Meakin (1983). The results for $2 \leq d \leq 6$ are summarized in Table 6.1. Several conclusions can be made from this Table. First, it appears that for all d considered, the following inequalities hold

$$d - 1 < D < d. \tag{6.4}$$

These values are in good accord with the mean-field prediction $D = (d^2 + 1)/(d + 1)$ to be discussed in Section 6.1.3.

Table 6.1. The fractal dimension (D) of DLA clusters grown on $2 \leq d \leq 6$ dimensional hypercubic lattices. The mean-field prediction $D = (d^2+1)/(d+1)$ is also shown for comparison (Meakin 1983a).

d	D	$(d^2 + 1)/(d + 1)$
2	1.70 ± 0.06	1.667
3	2.53 ± 0.06	2.500
4	3.31 ± 0.10	3.400
5	4.20 ± 0.16	4.333
6	5.3	5.286

The numerical result (6.4) can be supported by an argument providing a *lower bound* for the fractal dimension of diffusion-limited aggregates (Ball and Witten 1984a). Consider a system of randomly diffusing particles making one step in unit time, whose number density is ρ. Let us imagine the trajectories of these particles as they would have been in the absence of the aggregate. The density of individual steps after time t is ρt, while the

average number of virtual contacts with the aggregate is $N(t)\rho t$, where $N(t)$ is the actual number of particles in the DLA cluster. Next we want to estimate the average number of contacts of one trajectory with the aggregate. To obtain this quantity we recall that the trail of a randomly walking particle is a fractal of dimension 2 for $d \geq 2$ (Section 5.4.1). According to the related rule given in Section 2.3.1., the fractal dimension of the intersection of two fractals of dimensions D and 2 embedded into a d dimensional space is

$$D_\cap = D + 2 - d. \tag{6.5}$$

Correspondingly, the average number of contacts per trajectory goes as $R^{D_\cap}$, where R is the radius of the aggregate.

If $D_\cap > 0$, a typical trajectory intersects the aggregate many times. The number $A(t)$ of first contacts between trajectories and the aggregate is the total number of contacts divided by the number of contacts per trajectory

$$A(t) \sim \frac{N(t)\rho t}{R^{D+2-d}} \sim \rho t R^{d-2}. \tag{6.6}$$

The increase of $N(t)$ in unit time is the same as the total flux onto the aggregate which is equal to the time derivative of $A(t)$. Thus, $dA(t)/dt = dN(t)/dt = (dN(t)/dR)(dR(t)/dt)$. Inserting (6.6) and $N \sim R^D$ into this identity one gets

$$\rho R^{d-1+D} \sim dR(t)/dt. \tag{6.7}$$

Because of causality the growth speed $dR(t)/dt$ has to remain finite in the limit $R(t) \to \infty$, implying the inequality (6.4) we wanted to derive. If the assumption $D_\cap > 0$ we made earlier is violated, the aggregate is transparent to the particles, and the growth occurs nearly equally over the entire aggregate. In this way the density has to increase up to a point when $D_\cap$ becomes larger than zero and the above considerations hold.

In addition to its dependence on d, the fractal dimension may be affected by other factors. It is well known from the theory of critical phe-

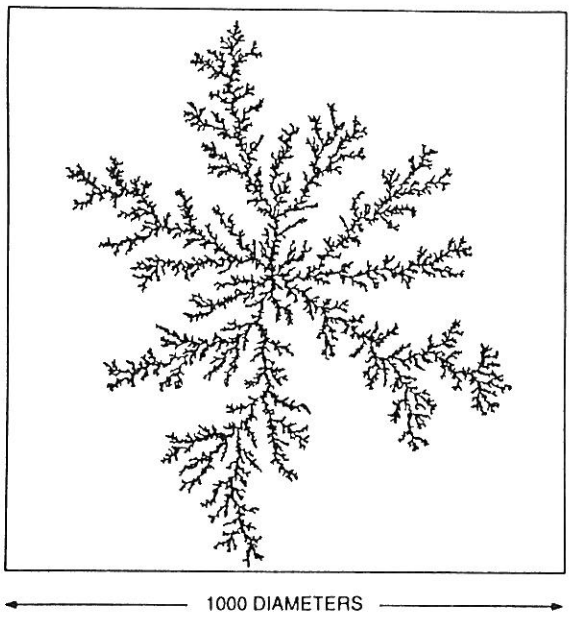

Figure 6.3. A typical off-lattice DLA cluster of 50,000 particles. A comparison with Fig. 6.1 showing a much smaller aggregate illustrates the stochastic self-similarity of diffusion-limited aggregates (Meakin 1985b).

nomena that the exponents describing the singular behaviour of quantities at a second order phase transition are not changed under the influence of irrelevant parameters such as anisotropy, further neighbour interactions, type of lattice, etc. This property of the exponents, called universality, is of special importance. The *question of universality* of the fractal dimension has been addressed in the context of DLA as well, by investigating modifications of the original model.

As a first approximation to this problem the following versions of diffusion-limited aggregation were considered (Witten and Sander 1983, Meakin 1983).

i) DLA with *sticking probability* less than 1. In this variation the particles stick to the surface with a probability p_s, and continue to diffuse with a probability $1 - p_s$.

ii) DLA with *next-to-nearest neighbour* interaction. In this version the particles stop moving as soon as they arrive at a site which is next nearest neighbour to the aggregate.

iii) *Off-lattice* DLA. During the simulations of this variant the centre of a diffusing spherical particle is moved with the same probability to any point within a distance equal to the diameter of the particles. If a particle is found to overlap with another one, the particle is moved back to the position where it first touched the cluster and is incorporated into the aggregate. Fig. 6.3 shows an off-lattice DLA cluster of 50,000 particles. This picture demonstrates *stochastic self-similarity* of diffusion-limited aggregates when one compares it with the much smaller aggregate in Fig. 6.1.

The results are given in Table 6.2 (Meakin 1983a). It is clear from the comparison of Tables 6.1 and 6.2 that the above mentioned modifications are irrelevant from the point of view of fractal dimension, at least for the sizes considered. However, as we shall see later, anisotropy plays a relevant role in the structure of aggregates. Among other effects, this will be manifested in the dependence of the large scale structure of aggregates on the type of lattice which is used in the simulations, making the question of universality a delicate problem.

Table 6.2. Fractal dimension (D) of DLA clusters grown using modified versions of the diffusion-limited-aggregation model. The notation is the following: p_s – sticking probability, $o-l$ – off-lattice, d – embedding dimension and nnn – sticking at next nearest neighbours. If not indicated, $p_s = 1$ and nearest neighbour interaction is used on the square and simple cubic lattices. These results should be compared with those presented in Table 6.1 (Meakin 1983a)

Model	D
d=2, p_s=0.25	1.72 ± 0.06
d=2, o-l	1.71 ± 0.07
d=2, nnn	1.72 ± 0.05
d=3, p_s=0.25	2.49 ± 0.12
d=3, o-l	2.50 ± 0.08

The above results seem to be consistent with the picture of a perfectly

self-similar DLA cluster. However, several observations (some of them discussed in the next section) indicate that the structure of diffusion-limited aggregates is more complex and the fractal dimension itself is not enough to characterize its scaling properties. The first result suggesting deviations from a standard behaviour was related to the width of the region (active zone) where the newly arriving particles are captured by the gowing cluster. The *active zone* can be well described in terms of the growth probability $P(r, N)$ which is the probability of the event that the Nth particle is attached to a cluster at a distance r from the origin (Plischke and Rácz 1984).

According to the simulations, $P(r, N)$ can be well approximated by a Gaussian characterized by two parameters $\bar{r}_N$ and ξ_N, representing the average deposition radius and the width of the active zone, respectively. For self-similar growth one expects that for $P(r, N)$ a scaling form analogous to (5.12) holds, i.e., $\bar{r}_N$ and ξ_N diverge with the same exponent as $N \to \infty$. Instead, simulations of DLA up to cluster sizes $N \sim 4000$ suggest that (Plischke and Ràcz 1984)

$$\bar{r}_N \sim N^{\nu} \qquad \text{and} \qquad \xi_N \sim N^{\nu'} \tag{6.8}$$

with $\nu = 1/D$ as expected, but with $\nu < \nu'$ in contradiction with the assumption of a single characteristic scaling length typical for the cutoff behaviour of a finite-size self-similar object. This conclusion may not hold in the asymptotic limit, since simulations of considerably larger off-lattice aggregates indicated that ν' tends to approach ν as $N \to \infty$ (Meakin and Sander 1985). Therefore, it appears that an extremely *slow crossover* takes place in the surface structure of DLA clusters as they grow. Similar observations have been made in the context of anisotropy of cluster shapes induced by the underlying lattice.

Finally, we briefly discuss numerical results obtained for the fractal dimension from a *Monte Carlo position-space renormalization* (PSRG) group approach (Montag *et al* 1985). This method is reviewed in Section 4.3. for growth processes in general. When applying the renormalization transformation (4.22) one has to determine the sum of probabilities $P_{N,i'}$ taken over

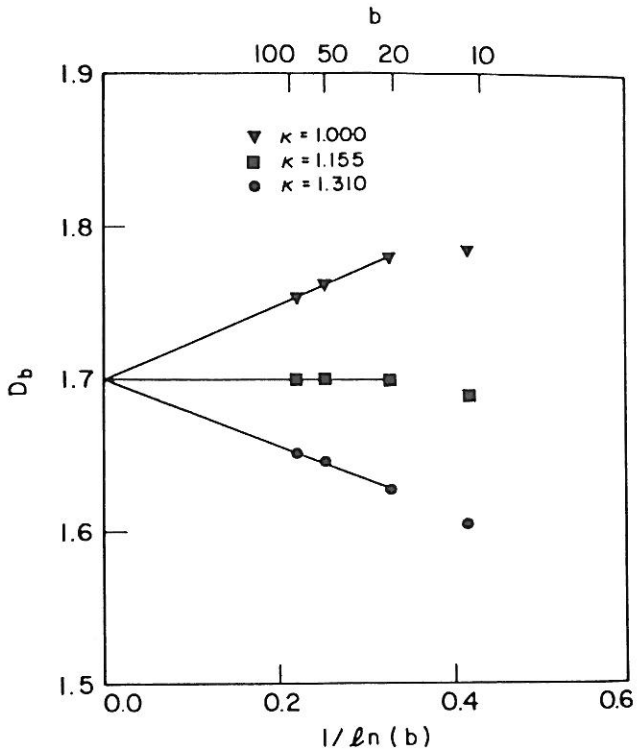

Figure 6.4. Extrapolation of the fractal dimension estimates, D_b, obtained from the phenomenological renormalization method to the large cell size ($b \gg 1$) limit. The calculations were carried out for three different values of the optimization parameter κ (Montag *et al* 1985)

i' from Monte Carlo simulations, where $P_{N,i'}$ is the probability that the i'th configuration consisting of N particles has a radius of gyration R_g such that $\kappa R_g = b/2$. Here κ is an optimization parameter (Vicsek and Kertész 1981) and b is the linear size of the cell renormalized into a single site. In practice, DLA clusters are grown from the centre of a cell and one records the number of sites in the cluster when its radius of gyration becomes equal to the cell size. Then the number of such occurrences is determined as a function of the number of sites in the cluster at that time. The data are fitted to a Gaussian, and the resulting curve is integrated to obtain Monte Carlo estimates of the coefficients in the renormalization transformation. Having determined $\sum_{i'} P_{N,i'}$ the eigenvalue (λ) of the transformation (4.22) is calculated numerically, and the fractal dimension is obtained from (4.25). Fig. 6.4 demonstrates that an extrapolation of the fractal dimension values D_b

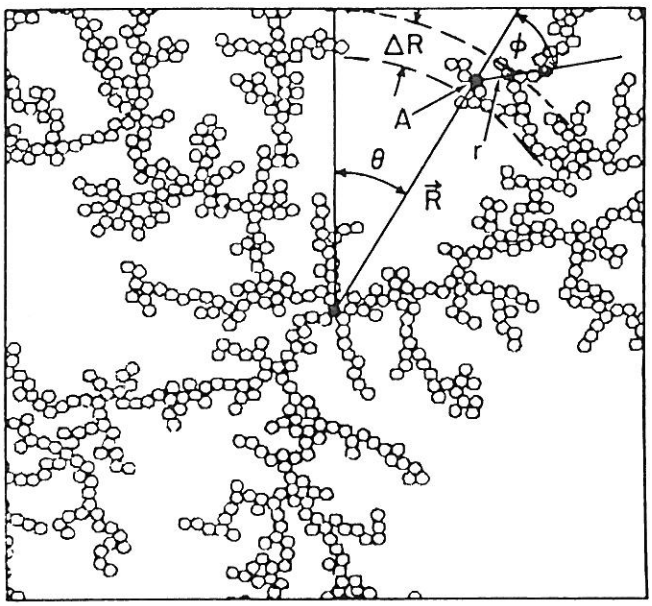

Figure 6.5. Central part of an off-lattice DLA cluster. The tangential correlations as a function of the angle θ are determined in a layer of width δR being at a distance R from the centre (Meakin and Vicsek 1985).

obtained for a given cell size b to the $b \to \infty$ limit provides accurate estimates of D in spite of the relatively small cluster sizes used in the calculations.

6.1.2. Anisotropy in DLA

While an ordinary stochastic fractal has an isotropic internal structure, this is not true for diffusion-limited aggregates which are isotropic only in a crude approximation. The determination of fractal dimension alone does not allow us to get an insight into the structural details of DLA clusters, although they are of interest, since one expects that the diffusion-limited mechanism has a very specific impact on the correlations and interrelation of branches inside an aggregate.

To see this one calculates the tangential correlation function $c_R(\theta)$ defined in $d = 2$ by (Meakin and Vicsek 1985, Kolb 1985)

$$c_R(\theta) = \frac{1}{N} \sum_{\theta'} \rho_R(\theta + \theta')\ \rho_R(\theta'), \tag{6.9}$$

where N is the number of particles in the aggregate, $\rho_R(\theta) = k$ if there are k particles in a box of size $R\Delta\theta\Delta R$ at the point (R, θ) and $\rho_R(\theta) = 0$ otherwise. The summation in (6.9) is taken over θ' values gradually increased by a fixed small $\Delta\theta'$ from $\theta' = 0$ to $\theta' = \pi$. According to (6.9), $c_R(\theta)$ describes the density-density correlations in a layer of width ΔR being at a distance R from the origin (Fig. 6.5) as a function of the angle θ measured from the origin of the clusters, so that θR is the distance separating two particles in the layer.

The results obtained for off-lattice aggregates are shown in Fig. 6.6. A finite size scaling analysis shows that asymptotically the tangential correlation function for $\theta \ll 1$ scales as a function of θ with an exponent $\alpha_\perp \simeq 0.41$. This exponent is definitely different from $\alpha \simeq 0.29$ which describes the algebraic decay of the ordinary radial correlation function (2.14).

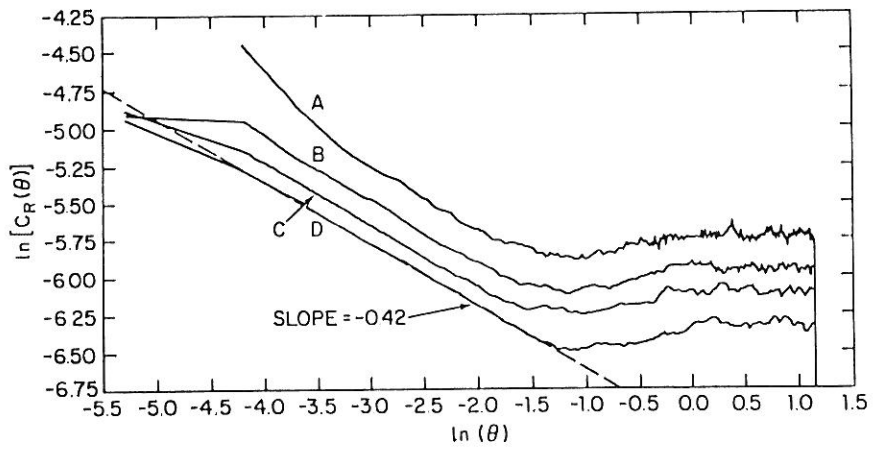

Figure 6.6. Tangential correlations in off-lattice DLA clusters of 50,000 particles. The results were obtained by averaging over the interval $\delta R = R \pm 0.05R$, where for the curves $A - D$ the radius R was respectively equal to 75, 150, 225 and 300 (Meakin and Vicsek 1985).

It follows from $\alpha_\perp > \alpha$ that the density correlations around a particle being at point $\vec{\mathbf{R}}$ depend on both r (denoting the distance from the given

particle) and the local angle φ, where $\varphi = 0$ in the radial direction $\vec{\mathbf{R}}$ as it is shown in Fig. 6.5. Let us assume that the density correlation function has the form

$$c(r,\varphi) \simeq \rho_0 r^{-\alpha_\parallel} \cos^2\varphi + \rho_1 r^{-\alpha_\perp} \sin^2\varphi, \tag{6.10}$$

where ρ_0 and ρ_1 are constants and $\alpha_\parallel$ describes the decay of $c(r,\varphi)$ in the radial direction. The relation (6.10) provides a simple example for a function with a power law decay consistent with the numerical data. Using (6.10) for the calculation of the fractal dimension in a manner analogous to (2.17) we get

$$N(a) \sim \int_0^a r dr \int_0^{2\pi} c(r,\varphi) d\varphi \sim \pi a^{2-\alpha_\parallel} (\rho_0 + \rho_1 a^{\alpha_\parallel - \alpha_\perp}), \tag{6.11}$$

where $N(a)$ is the number of particles within a circle of radius a. The fractal dimension is given by

$$D = \lim_{a\to\infty} \frac{\ln N(a)}{\ln a} = \lim_{a\to\infty} 2 - \alpha_\parallel + D_1(a) = 2 - \alpha_\parallel \tag{6.12}$$

with $D_1 = [\ln \pi(\rho_0 + \rho_1 a^{\alpha_\parallel - \alpha_\perp})]/\ln a$ representing a slowly decaying correction to scaling (Meakin and Vicsek 1985).

The main conclusions one can draw on the basis of the above results are the following: i) diffusion-limited aggregates are *not isotropic self-similar* fractals, instead, they possess a special kind of self-affinity with direction dependent scaling of the density correlations, ii) The fractal dimension is determined by the exponent describing the decay of radial correlations, and finally, iii) the observed slow convergence of D to its asymptotic value is due to the correction term D_1 related to $\alpha_\perp$.

The above discussed anisotropy originates in the fact that DLA clusters grow by developing branches oriented away from a fixed origin. This type of symmetry shows up in the behaviour of the *three point correlation function* as well (Halsey and Meakin 1985). The results of the related simulations indicate that while the decay of $c(r)$ is determined by the same exponent

throughout the cluster the structure is not homogeneous. In particular, the amplitude of the power law decay at points close to the origin is larger than elsewhere.

Another kind of anisotropy is manifested in the studies of the *overall shape* (or envelope) of DLA clusters. Results concerning the response of diffusion-limited aggregates to anisotropy show that the anisotropy of both the underlying lattice and the sticking probability represents a relevant parameter changing the general appearance of DLA clusters drastically.

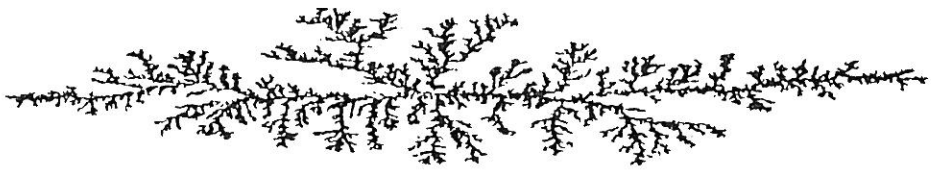

Figure 6.7. A representative DLA cluster grown using anisotropic sticking probability (Ball *et al* 1985).

One way to impose anisotropy is to make the sticking probability direction dependent (Ball *et al* 1985). This can be achieved on a square lattice by differentiating between two possible cases: i) the particle sticks with probability 1 if the left or right nearest neighbour sites to its actual position are occupied, ii) otherwise, it only has a probability $p_s < 1$ of sticking. This modified version of DLA leads to highly elongated clusters, as it can be seen in Fig. 6.7. According to the simulations the characteristic lengths of the aggregate X and Y in the easy (x) and hard (y) direction of growth increase as $X \sim N^{\frac{2}{3}}$ and $Y \sim N^{\frac{1}{3}}$ in the limit $N \to \infty$. Since $X \times Y \sim N$, the area covered by the cluster grows linearly with N which means that for any applied uniaxially anisotropic sticking probability the cluster will eventually grow into an object homogeneous on a large scale. All of these findings are in accord with a theoretical approach discussed in the next Section.

Although relatively small DLA clusters grown on various lattices of the same dimension were found to have the same radius of gyration exponent ν,

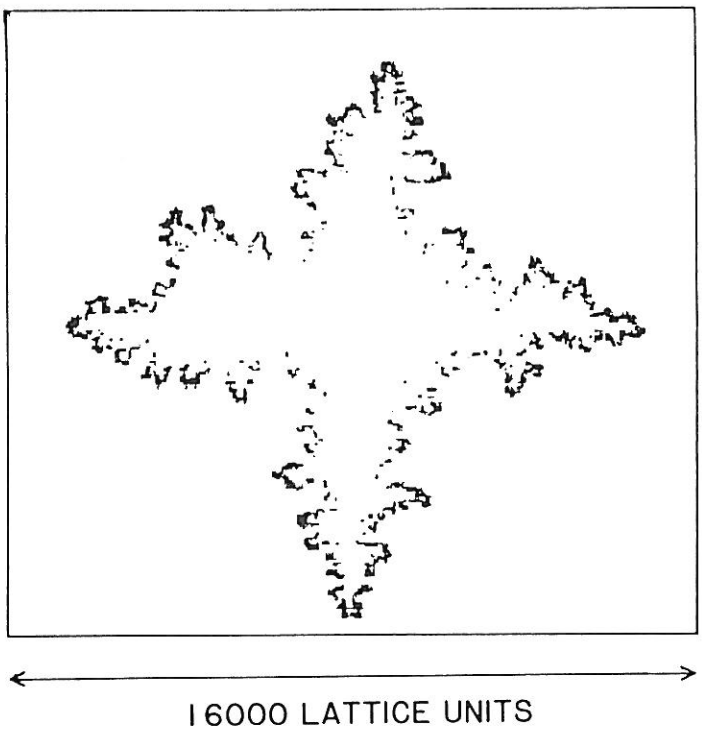

Figure 6.8. Envelope of a very large DLA cluster (consisting of 4×10^6 particles) generated on the square lattice. The effect of the lattice anisotropy is shown by plotting the last 2×10^5 particles attached to the cluster (Meakin *et al* 1987).

simulations carried out on a larger scale indicated that the symmetry of the underlying lattice may affect the asymptotic behaviour of aggregates. Growth on the square lattice was studied in more detail from this point of view, and the results confirmed the *relevant role of the lattice anisotropy* (Meakin *et al* 1987) .

In order to see how the crossover to the $N \to \infty$ regime takes place particularly large clusters (consisting of 4×10^6 particles) have to be generated using the algorithm described in Appendix A. The anisotropy of the resulting cross-like structures can be demonstrated by plotting only the regions where the last 2×10^5 particles were added to the cluster. Fig. 6.8 shows a typical configuration of these active places visualizing the envelope of a very large diffusion-limited aggregate. It is apparent from this figure that as DLA clusters grow larger their shape becomes more similar to that associated with conventional *dendritic growth* which is known to be governed by the anisotropy of the surface tension.

The above observation can be made quantitative by determining the characteristic sizes of the four main arms of the cross-like structure (Meakin *et al* 1987). Let us define the exponents $\nu_{||}$ and $\nu_{\perp}$ through the scaling of the average length

$$l \sim N^{\nu_{||}} \tag{6.13}$$

and average width

$$w \sim N^{\nu_{||}} \tag{6.14}$$

of the arms as a function of the number of particles in the clusters, N. The quantity l can be estimated from the maximum of the cluster radius, while w can be associated with the mean deposition distance from the nearest of the lattice axes (crossing at the origin). The crossover to the behaviour corresponding to (6.13) and (6.14) is particularly *slow*. However, approximating the behaviour of R_{max} with a curve of the form

$$R_{max} = aN^{\nu_{||}}(1 + bN^{-\Delta}) \tag{6.15}$$

provides a relatively good fit to the data with $\nu_{||} = \frac{2}{3}$ and with some constants a, b and Δ not relevant from the present point of view. A similar analysis for X gives $\nu_{\perp} \simeq 0.48 \simeq \frac{1}{2}$. These results correspond to at least two independent length scales describing the large scale behaviour of DLA clusters and, correspondingly, one expects that

$$w/l \to 0 \qquad \text{for} \qquad N \to \infty. \tag{6.16}$$

The above expression means that the angle at the tip of an arm should go to zero in the asymptotic limit. This angle plays an important role in a theoretical approach (next Section) based on solving the Laplace equation for a region surrounding a tip of idealized geometry. According to this theoretical model the rate of growth at the maximum radius is determined by the angle

θ through $dR_{max}/dN \sim R_{max}^{-\pi/2\varphi}$, where $\pi - \varphi$ is half of the tip angle. The dependence of φ on $\ln N$ as determined from the simulations is surprisingly linear, but it is not inconsistent with limiting values of $\leq 180°$ (thin cross) for large N and $\simeq 27°$ ($D \simeq 1.70$) for relatively small N. However, it should be pointed out that the investigation of the noise-reduced version of DLA (Section 9.2.2.) indicates that (6.16) may be violated for sizes which are beyond those accessible by direct simulation.

The discussion of lattice induced anisotropy raises the question of the asymptotic shape of DLA clusters grown on other lattices. According to the simulations on the triangular and hexagonal lattices no signs of a crossover to a star-like overall form could be observed up to cluster sizes of 80,000 particles. The values obtained for the fractal dimensions indicat that diffusion-limited aggregates generated on these lattices have fractal dimensions numerically indistinguishable off-lattice DLA clusters (Meakin 1987).

These results suggest that during the process of aggregation there is a *competition* between anisotropy (provided by the lattice) and randomness (due to the stochastic motion of the particles) both having a relevant impact on the asymptotic behaviour (more about such questions can be found in Section 10.1.2.). The triangular lattice is not anisotropic enough (it has too many axes) to force an arm to grow in a given direction. Consequently, there seems to exist an upper limit for the number of distinct main arms growing out from the central region of a diffusion-limited aggregate. This problem can be attacked by introducing various kinds of anisotropies and estimating the number of arms which can grow in a more or less stable fashion. The present consensus is that in the asymptotic limit diffusion-limited aggregates are not likely to have more than 5 main arms in two dimensions. In particular, off-lattice DLA clusters might acquire the shape of a 4 or 5 fold star as $N \to \infty$ (Ball 1986, Meakin and Vicsek 1987). However, up to sizes simulated so far, the overall shape of an off-lattice aggregate (like those generated on the triangular and hexagonal lattices) does not seem to deviate from a circle significantly.

6.1.3. Theoretical approaches to DLA

Diffusion-limited aggregation is a far from equilibrium phenomenon with no standard theory founded on first principles only. The approaches discussed in this Section are based on various assumptions depending on the particular theoretical model considered. The most relevant difficulty is to take into account the spatial fluctuations characteristic for a DLA cluster in an appropriate way. This problem is usually treated by assuming some kind of average behaviour for such properties of a cluster as the distribution of its density, the penetration length of an incoming particle, or the aggregate's envelope.

There are two main types of *mean-field* approach to DLA. The first class is analogous to that introduced by Flory (1971) to describe the structure of linear polymers. In the Flory approximation one calculates the free energy of a cluster as a function of N and its linear size neglecting density fluctuations. Then the fractal dimension is obtained from the condition that the free energy has to be minimal. For a far from equilibrium system the construction of free energy and its minimalization do not represent well founded principles. However, following this line it is possible to obtain for the fractal dimension a simple expression (Tokuyama and Kawasaki 1984)

$$D = \frac{d^2 + 1}{d + 1} \tag{6.17}$$

which gives values surprisingly close to the simulation results.

An alternative method is to express the growth rate of a DLA cluster through the *screening or penetration length* ξ, where ξ is the average depth of the layer at the surface of a cluster which is accessible for an incoming particle (Muthukumar 1983). In fact, the result (6.17) was first obtained by this approach. As an example of such mean-field theories let us consider the following heuristic argument (Honda *et al* 1986). We assume that the particles follow a trajectory of dimension D_w (it can be a Levy walk or walk on a fractal, see previous Chapter) and for convenience denote the number of particles in a layer of width dr being at a distance r from the origin by

which reduces to (6.17) for $D_w = 2$. For $d = 1$ (ballistic aggregation) the above expression yields $D = d$ in accord with other results. The comparison of (6.23) with estimates obtained by other approaches for various d and d_w values leads to reasonable agreement as well.

Investigation of the *growth probability scaling near the tips* of the clusters represents an important and far reaching contribution to the theoretical description of diffusion-limited aggregation (Turkevich and Scher 1985, Ball *et al* 1985). In this approach the analogy between the probability of finding a particle at a given point close to an array of traps and the distribution of electrostatic potential ϕ around a conductor (see Section 9.1.) is utilized.

Consider a DLA cluster of N particles having a maximum radius R. The probability of finding a diffusing particle in a certain site $\vec{\mathrm{r}}$ outside the cluster satisfies the Laplace equation $\nabla^2 p(\vec{\mathrm{r}}) = 0$ with the boundary condition $p = 0$ on sites adjacent to the cluster. The flux of particles onto the cluster at a point $\vec{\mathrm{r}}_0$ on its surface is proportional to $\nabla p(\vec{\mathrm{r}}_0)$. The electrostatic analog of this problem is a charged conductor having the shape of a cluster. In particular, the local electric field $\vec{\mathrm{E}} = -\nabla\phi$ (or the surface charge density) is the analog of the flux of particles $dR/dt = (dN/dt)/(dN/dR)$ onto that point, where dN/dt is the total flux of particles onto the cluster corresponding to the total charge, and $dN/dR \sim R^{D-1}$.

Clearly, if one is able to obtain an expression for dN/dR from electrostatics, comparison with the above relation for the same quantity should provide an estimate for D. It is quite natural to assume that the most advanced parts of a cluster (where the deposition of the particles takes place) can be represented by a cone of exterior half angle φ (Fig. 6.9). This is an idealization of the actual situation, however, it reflects one of the basic properties of DLA clusters: the active surface consists of advanced tips corresponding to a local singularity of both the geometry and the deposition probability.

The problem of finding the solution of the Laplace equation for a conducting infinite cone can be solved exactly via conformal transformation giving

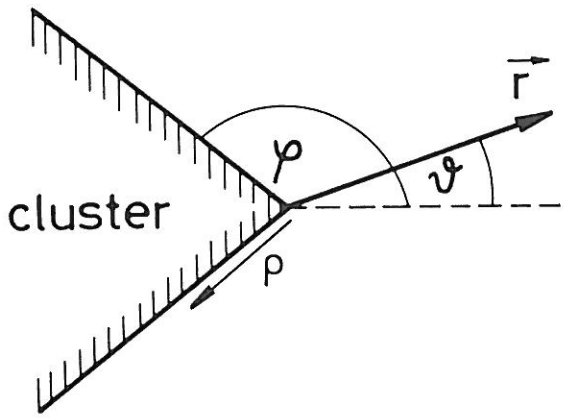

Figure 6.9. Modelling the region around the tips of DLA clusters with a cone of exterior half angle φ.

$$\phi(r,\vartheta) = C\ r^{\pi/(2\varphi)} \cos(\pi\vartheta/2\varphi), \tag{6.24}$$

where C is a normalization factor. Thus the steady-state flux of diffusing particles onto the cone edge at a distance λ from its tip is

$$\nabla\phi(\lambda,\varphi) = \frac{C\ \pi}{2\varphi}\lambda^{\pi/(2\varphi)-1}. \tag{6.25}$$

One obtains dN/dt by integrating the above expression from $\lambda = 0$ to some large cutoff at $\lambda \sim R$ and dR/dt by integrating up to a small cutoff $\lambda \sim a$, where $a = 1$ is the size of diffusing particles or the lattice spacing. We find from (6.25) that $dN/dt \simeq C\ R^{\pi/(2\varphi)}$ and $dR/dt \simeq C$ which leads to

$$\frac{dN}{dR} = \frac{dN/dt}{dR/dt} \simeq R^{\pi/(2\varphi)}. \tag{6.26}$$

Integrating the above expression gives for the fractal dimension

$$D = 1 + \frac{\pi}{2\varphi} = \frac{3\pi - \theta}{2\pi - \theta} \tag{6.27}$$

which is the main result of the probability scaling approach in two dimensions

$$\rho(r)dr = \frac{dn(r)}{dr}dr \sim r^{D-1}dr, \tag{6.18}$$

where $n(r)$ is the number of particles within a sphere of radius r. Suppose that $\Delta N \ll N$ new particles are added to the cluster. Then the cluster radius increases by ΔR so that

$$N + \Delta N \sim (R + \Delta R)^D. \tag{6.19}$$

Since $N + \Delta N \sim \int_0^{R+\Delta R}[\rho(r) + \delta\rho(r)]dr$, from (6.18) and (6.19) we get for the increment of the number of particles within a shell at a distance r from the origin

$$\delta\rho(r) \sim r^{D-1} \tag{6.20}$$

with a coefficient proportional to ΔN. Next one makes the heuristic assumption that this increase of $\rho(r)$ is proportional to the volume of the empty regions in which the particles can diffuse before deposition

$$\delta\rho(r) \sim \xi^d(r). \tag{6.21}$$

To proceed we need to obtain an estimate for ξ. This can be done by taking into account that a particle makes, on average, $N_w \sim \xi^{D_w}$ steps before hitting the cluster. The number of steps on the surface of this "cloud" of steps is then proportional to $N_{w,s} \sim \xi^{D_w-1}$. On the other hand, the average density of particles belonging to the cluster grows with r as $\sigma(r) \sim r^{D-d}$. From the condition that the actual deposition takes place when $N_{w,s}\sigma(r) \simeq 1$ one gets

$$\xi(r) \sim r^{(d-D)/(D_w-1)}. \tag{6.22}$$

The final result is obtained by comparing (6.20), (6.21) and (6.22)

$$D = \frac{d^2 + D_w - 1}{d + D_w - 1} \tag{6.23}$$

(Turkevich and Scher 1985).

Let us discuss the above results considering various assumptions for θ. In the previous Section DLA clusters with anisotropic sticking probability were shown to evolve into an elongated quadrangle becoming increasingly needle-like with growing N. This geometry corresponds to $\varphi_x = \pi$ and $\varphi_y = \frac{\pi}{2}$ in the limit $N \to \infty$, where φ_x and φ_y are exterior half angles of the cones oriented in the direction of easy growth (x) and hard growth (y), respectively. Then expressions analogous to (6.26) applied to the description of the tip distances in the x and y directions yield (Ball *et al* 1985)

$$X \sim N^{2/3} \qquad \text{and} \qquad Y \sim N^{1/3} \tag{6.28}$$

in complete agreement with the simulation results.

It is less clear what is the appropriate value of φ or θ in (6.24) when one is interested in D of ordinary diffusion-limited aggregates. The assumption $\theta = \frac{\pi}{2}$ corresponding to a growing square on the square lattice gives for the fractal dimension $D = \frac{5}{3}$, a good estimate coinciding with the prediction of the mean-field approach. For the unbiased off-lattice case there is no direct way to determine θ, and (6.27) can be regarded as a definition for an effective angle $\theta_{eff} \simeq 0.59\pi \simeq 106°$ through the known fractal dimension $D \simeq 1.71$.

The above method can be generalized to dimensions higher than $d = 2$ (Turkevich and Scher 1986). In this case the fractal dimension can be written in the form $D(d) = 2 + \omega$, where ω is the degree of the ordinary Legendre function, and it is determined from an implicit equation derived from the condition that the right-angled hypercone should be at zero potential. The case of d dimensional cross-shape clusters can also be described by this approach using $\theta = 0$ for the angle of the hypercone representing the tips of the needle-like arms of the aggregate. The corresponding result is

$$\omega = \begin{cases} (d-3)/2, & \text{if } 1 \le d \le 3, \\ d-3, & \text{if } d \ge 3 \end{cases} . \tag{6.29}$$

Finally, it should be noted that a number of further approaches have been ap-

plied to the theoretical description of DLA. Position-space renormalization group (PSRG) (see Section 4.3.) represents a standard tool for calculating non-integer exponents characterizing the singular behaviour of various quantities in systems exhibiting equilibrium phase transitions (Stanley *et al* 1982). However, its application to DLA raises a number of unresolved questions, especially, when small cells are used (Gould *et al* 1983). Small cell renormalization has also been used to calculate the multifractal spectrum of growth probabilities (Nagatani 1987a, 1987b). In fact, the actual values for D are usually not accurate, and depend too strongly on the particular (sometimes quite arbitrary) rules assumed in the course of renormalization. In a different approach first the number of main arms m in a cluster was determined from a stability analysis (Ball 1986). Then this number was used to calculate D using the probability scaling theory, assuming that the cluster has a polygonal shape with m tips. Here it is not clear whether the shape of a cluster can be simultaneously associated with both a star-like object and a convex polygon. The scaling of the length and the width of the arms with N has also been addressed using conformal transformation and scaling arguments (Szép and Lugosi 1987, Family and Hentschel 1987).

6.1.4. Multifractal scaling

According to the simulations and the theoretical arguments discussed in the previous Sections the growth of a DLA cluster is governed by the distribution of the quantity $p(\vec{r}_j)$, where $p(\vec{r}_j)$ is the probability that the next growth event takes place at the site being at $\vec{r}_j$, adjacent to the cluster. This *growth-site probability distribution* (GSPD) is a very complex function changing rapidly in space due to screening (Halsey *et al* 1986, Amitrano *et al* 1986, Meakin *et al* 1986a). Let us imagine that we proceed along the surface of an aggregate and we record $p(\vec{r}_j)$ as a function of the arc length. Whenever we approach a tip in the outer region of the cluster, the growth probability associated with the actual position sharply increases since an advanced tip captures the diffusing particles with a large probability. Leaving this region one may get into a deep fjord which is almost completely screened by the surrounding branches, here $p(\vec{r}_j)$ is practically equal to zero. Getting close

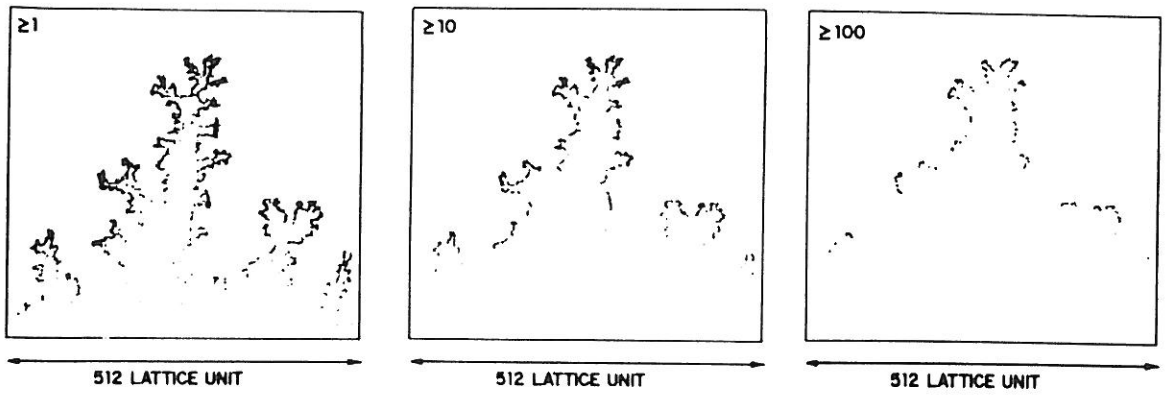

Figure 6.10. This figure shows those sites of a diffusion-limited deposit (grown on a strip of width 512 lattice units) which were contacted by the 5×10^5 random walk probes at least 1, 10 and 100 times (Meakin 1987a).

to another tip the growth probability becomes much larger again.

This is demonstrated in Fig. 6.10, where only those perimeter sites (sites adjacent to the aggregate) are shown which were hit by randomly walking probe particles at least 1, 10 and 100 times (Meakin 1987a). In general, the exponent describing the singular increase of $p(\vec{r}_j)$ depends on the local configuration close to a given tip. Therefore, it is quite natural to look at GSPD as a *fractal measure* (see Chapter 3.) with infinitely many types of singularities. Probing the surface with many random walks is equivalent to the estimation of the corresponding solutions of Laplace's equation (Section 9.1.) which are usually called harmonic functions. Consequently, the name harmonic measure is also used for GSPD.

In addition to describing the distribution of growth probabilities, the harmonic measure is relevant to the physical properties of a fractal. In the preceeding Section it was discussed that $p(\vec{r}_j)$ is proportional to the local charge density on a DLA, assuming that the aggregate is a charged electrical conductor. Similarly, the absorption rate of a DLA shaped catalyzer representing a sink for diffusing particles can be interpreted in terms of GSPD. Other physical processes may depend on the structure of the cluster in a different manner giving rise to fractal measures of various types associated with the aggregate. However, in most of the cases the freshly grown parts of

the aggregate determine its physical properties and those are the the corresponding fractal measures which provide a detailed description of this surface region.

To calculate the harmonic measure and its characteristic properties one can follow two numerical methods. i) After having generated a DLA cluster one releases further particles (Halsey *et al* 1986, Meakin *et al* 1986a) whose diffusional motion is simulated by the same technique (Appendix A) which is used for growing the aggregate. These probe particles, however, are eliminated when they arrive at the surface, and a record is kept of how many times each of the surface sites is contacted in this way. The normalized number of contacts is then regarded as the growth probability. The main disadvantage of this method is that it can only be used to obtain information about the harmonic measure in those regions where the measure is large enough (places with $p(\vec{r}_j) \ll 1$ are not visited by a sufficient number of trajectories). Consequently, only quantities determined by the positive moments of the probability distribution can be calculated.

Therefore, more complete data can be obtained by ii) solving the Laplace equation $\nabla^2\phi = 0$ with the boundary conditions $\phi = Const$ on the cluster and $\phi = 0$ far from it. Then the growth probabilities are given by $p(\vec{r}_j) \sim |\nabla\phi(\vec{r}_j)|$ on the basis of the electrostatic analog (preceeding Section). For small clusters the Green's function method can be used to solve Laplace's equation (Amitrano *et al* 1986) yielding GSPD free of any effects caused by the finite distance of the boundary with $\phi = 0$ from the aggregate. For larger clusters, which are usually needed to see the true scaling behaviour, it is more practical to solve the discrete version of the Laplace equation by relaxation methods (Hayakawa *et al* 1987).

After having determined the set of $p(\vec{r}_j)$ values, the generalized dimensions D_q and the $f(\alpha)$ spectrum of fractal dimensions corresponding to the singularities of strength α can be calculated using the expressions (3.11), (3.13) and (3.16) given in Chapter 3. For this purpose one has to cover the cluster with boxes of size l and sum up the $p(\vec{r}_j)$ values within the ith box to obtain the accumulated probability p_i associated with it. Then the exponent describing the scaling of the qth moment of the harmonic measure is given

by

$$D_q = \lim_{l/L \to 0} \frac{1}{q-1} \frac{\ln \sum_i [p_i(l/L)]^q}{\ln(l/L)}, \tag{6.30}$$

were L is the linear size of the aggregate. To evaluate (6.30) one can either change l for a fixed cluster, or keep $l = 1$ and consider the growth probabilities for increasing L values. Note, that in principle both of the conditions $a/l \ll 1$ and $l/L \ll 1$ should be satisfied during the calculations to produce results exactly corresponding to the multifractal spectrum as defined for finite fractals (with no lower cutoff length scale). In practical calculations these conditions can not be satisfied because of computer time and memory limitations. Due to (6.30) the log-log plots of $\sum_i p_i^q$ versus l/L have a slope $(q-1)D_q$ providing an esimate for the generalized dimensions. Fig. 6.11 shows the results for two-dimensional off-lattice aggregates (Hayakawa *et al* 1987).

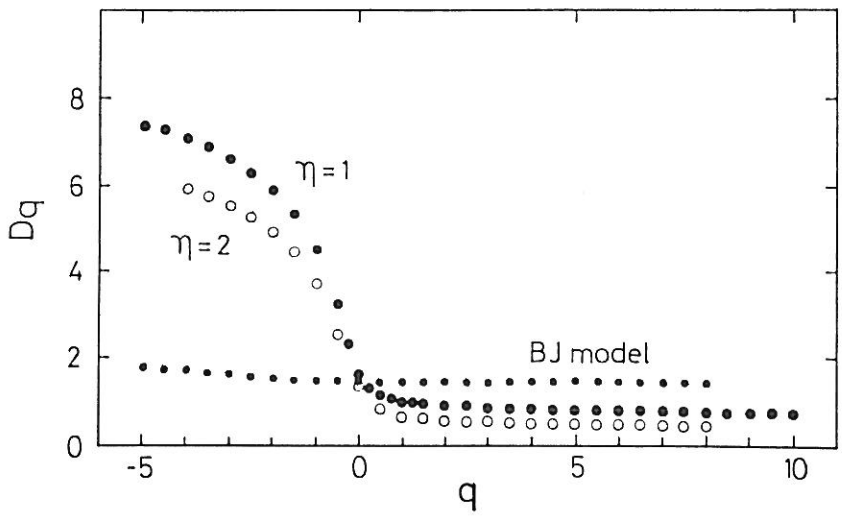

Figure 6.11. The generalized dimensions D_q calculated for off-lattice DLA clusters consisting of 3000-70000 particles ($\eta = 1$). The data obtained for the dielectric breakdown model ($\eta = 2$) and the disaggregation model (BJ) will be discussed in Sections 6.2 and 6.3 (Hayakawa *et al* 1987).

The obtained estimates can be examined using a few theoretical predic-

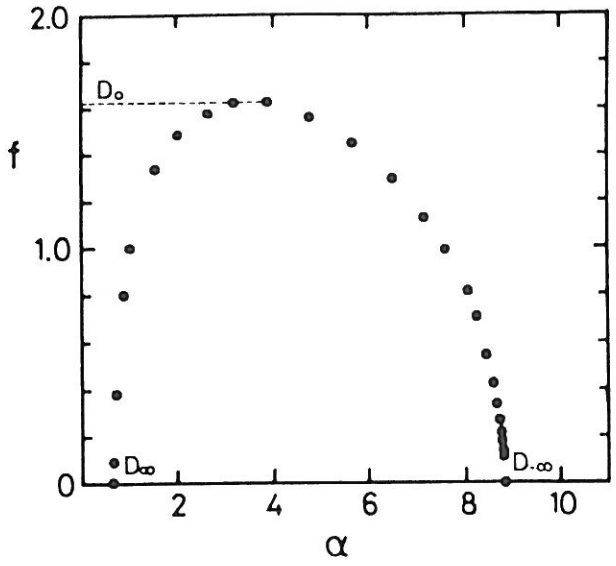

Figure 6.12. The spectrum of fractal dimensionalities, $f(\alpha)$, for the growth site probability distribution of off-lattice DLA clusters (Hayakawa *et al* 1987).

tions. The value D_1 called information dimension has particular importance. It is equal to the fractal dimension of the set of boxes which give the dominant contribution to the first moment, i.e., to the sum of the box probabilities. According to a recent mathematical theorem, in $d = 2$ the information dimension of the harmonic measure is equal to 1 (Makarov 1985), therefore, most of the measure is concentrated on a fractal of dimension $D_1 = 1$. Furthermore, the exponent of the $q = 0$th moment has to be equal to the fractal dimension of the substrate on which the measure is defined. These predictions are consistent with the numerical data of Fig. 6.11: $D_0 \simeq 1.64$ ($D_{DLA} \simeq 1.7$) and $D_1 \simeq 1.04$). Finally, $D_3 \simeq 0.85$ is in good agreement with a recent theoretical result implying for DLA $2D_3 = D$ (Halsey 1987).

The $f(\alpha)$ spectrum can be determined through the Legendre transformation of D_q according to the expressions (3.13 – 3.15). The result is presented in Fig. 6.12. This continuous function demonstrates that the harmonic measure divides a DLA cluster into interwoven fractal subsets with dimensions between $0 < f(\alpha) < D_0 = D$ each characterized by the corresponding singularity of strength $\alpha_\infty < \alpha < \alpha_{-\infty}$.

The top of the curve in Fig 6.12 is at $D_0 = D \simeq 1.62$ in reasonable

agreement with the simulations aimed at calculating the fractal dimension only. Another possibility for comparison with theoretical results is provided by expression (6.27) connecting the fractal dimension of the cluster with the effective angle of the cone representing the tip of an advanced branch. Writing (6.27) in the form $D = 1 + x$ and (6.25) as $\nabla\phi \sim l^{x-1}$ one can see that the integral of $\nabla\phi \sim p_i$ (which is the accumulated probability in a box of size l placed onto a tip) scales with the exponent x. Thus, assuming that the fractal dimension is determined by tips having the strongest singularity one obtains

$$D = 1 + \alpha_{\infty}. \tag{6.31}$$

The value $\alpha_{\infty} \simeq 0.7$ in Fig. 6.12 is in good accord with the above prediction ($D \simeq 1.7$).

The definitions (3.2) and (3.3) allows one to make an attempt to plot $f(\alpha)$ directly from the data obtained for the growth probabilities $p(\vec{r}_j)$. Assuming $l = a = 1$ and using as a measure of the linear size $M^{1/D} \sim L$ instead of L one can combine (3.2) and (3.3) to give

$$\frac{\ln[pN(p)]}{\ln M} \sim f\left(\frac{\ln p}{\ln M}\right), \tag{6.32}$$

where $pN(p)d\ln p = [dN(\ln p)/d\ln p]\ln p$ is the number of sites with growth probabilities between $\ln p$ and $\ln p + d\ln p$ with $dp \ll 1$. If there exists a unique scaling function $f(\alpha)$, the data obtained for $\ln[pN(p)]/\ln M$ plotted against $\ln p/\ln M$ for various M should fall onto the same curve. Of course, this procedure should give the right exponents only if the approximation $l = 1$ can be justified. Very recent results indicate that the condition $l \gg a$ has to be satisfied to get reliable results, where a is the lattice constant.

In Fig. 6.13 the above scaling is tested using data for $pN(p)$ determined from probing the surface of two-dimensional DLA clusters with 10^6 diffusing particles (Meakin *et al* 1986a). The collapse of the results is not particularly good but clearly improves as the cluster mass increases. The maximum is close to 1.0 as expected, since it should be equal to $f(\alpha_{max}) = D$

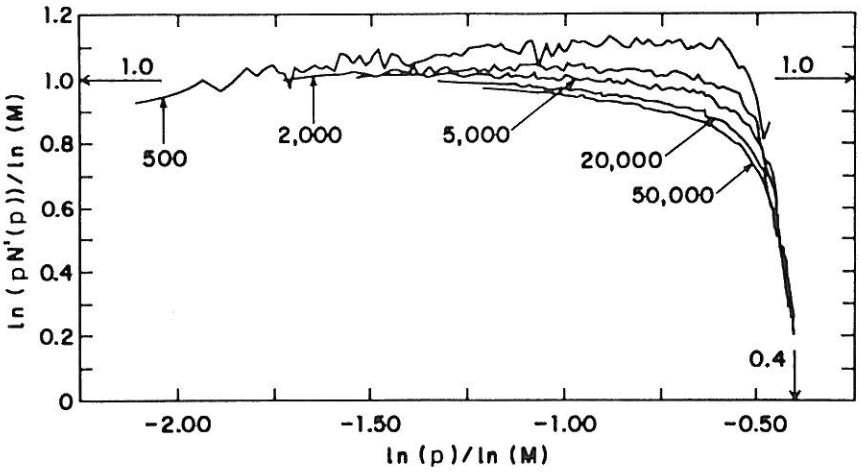

Figure 6.13. Result of an attempt to rescale the data for the growth probability distribution, $N(p)$, into a single curve corresponding to $D^{-1}f(\alpha)$ (Meakin *et al* 1986a).

when $\ln L = D^{-1} \ln M$ is used to represent the size of the system. It can also be seen in Fig. 6.13 that the maximum growth probability p_{max} scales with the size of the cluster according to

$$p_{max} \sim M^{-\delta} \tag{6.33}$$

with $\delta \simeq 0.4$ which is predicted by the probability scaling theory (preceding section) through the expression $\delta = 1 - 1/D$.

In Section 3.4. it has been shown that apart from the multifractal behaviour of a singular measure defined on a fractal, a fractal substrate itself can also exibit multifractal scaling of its mass. It is presently an open question of great interest whether randomly growing structures like DLA clusters are such geometrical multifractals. The first steps in the direction of treating this problem were concerned with the mass distribution in two-dimensional aggregates (Meakin and Havlin 1987).

To analyse the *mass distribution* one chooses a site randomly on a large off-lattice aggregate and determines $P_s(r)$ which is the probability of having s sites belonging to the cluster within a distance r of the given site. Then the fractal dimension is given by

$$\langle s \rangle = \int_0^\infty s P_s(r) ds \sim r^D. \tag{6.34}$$

Next we assume that $P_s(r)$ has the simplest scaling form yielding (6.34)

$$P_s(r) \sim \frac{1}{s} f\left(\frac{s}{r^D}\right), \tag{6.35}$$

where the factor s^{-1} is needed to satisfy the normalization condition of $P_s(r)$

$$\int_0^\infty P_s(r) ds = 1. \tag{6.36}$$

It is important to note that (6.35) is qualitatively different from the expression one would have for a homogeneous object, where the number of particles within a box of given size is described by the Poisson distribution. In the large r limit the Poisson distribution becomes delta function-like on a log-log plot, while (6.35) results in an invariant shape. If (6.35) is valid the moments of the distribution can be easily calculated (changing the variable of integration to $s = z/r^D$)

$$\langle s^q \rangle \sim \int_0^\infty s^{q-1} f(s/r^D) ds \sim r^{qD} \qquad \text{for } q > 0, \tag{6.37}$$

therefore, all of the positive moments can be expressed as powers of the first one.

However, the simulations of $2d$ off-lattice DLA ($D \simeq 1.7$) do not seem to lead to a satisfactory agreement with the above scaling picture based on the assumption of a single exponent D. Attempts to rescale $P_s(r)$ according to (6.35) onto a universal curve failed, as is shown in Fig. 6.14. The best collapse of the data was achieved using $P_s(r) \sim s^{-0.9} f(s/r^{1.57})$, which is clearly inconsistent with (6.35). In addition, the ratio $\langle s^q \rangle / \langle s \rangle^q$ was found to depend on r: another result indicating that the mass distribution within a DLA cluster can not be described by simple scaling of the type (6.35). Thus one is led to the conclusion that geometrical multifractality of DLA clusters should be investigated further with the help of the formalism given in Section

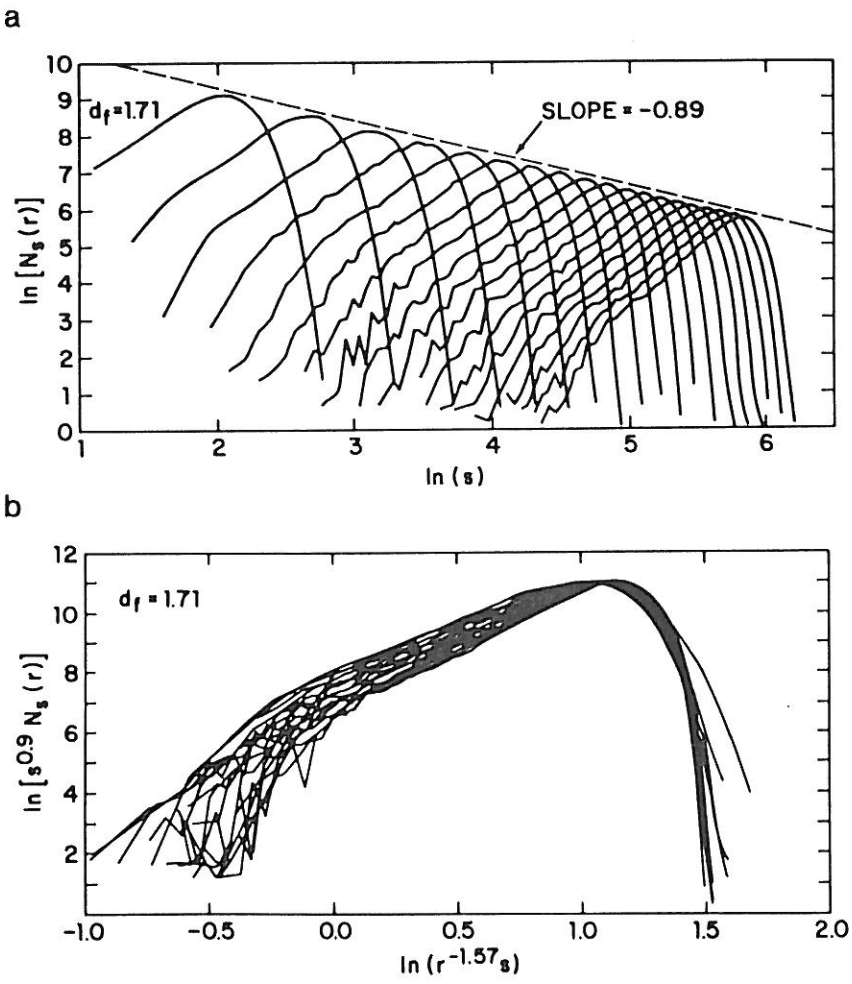

Figure 6.14. Attempt to scale the quantity $N_s(r) = N(r)P_s(r)$ determined for various r (a) into a single curve (b), where $N(r)$ is the total number of circles of radius r considered in the numerical experiment (Meakin and Havlin 1987).

in Section 3.4.

6.2. DIFFUSION-LIMITED DEPOSITION

The deposition of materials onto surfaces to form layers with specific properties has become an important technology with a very broad range of applications. In practice, deposition is carried out under conditions which allow various complex physical and chemical processes to occur. Diffusion-limited deposition (Meakin 1983b, Ràcz and Vicsek 1983) represents a rele-

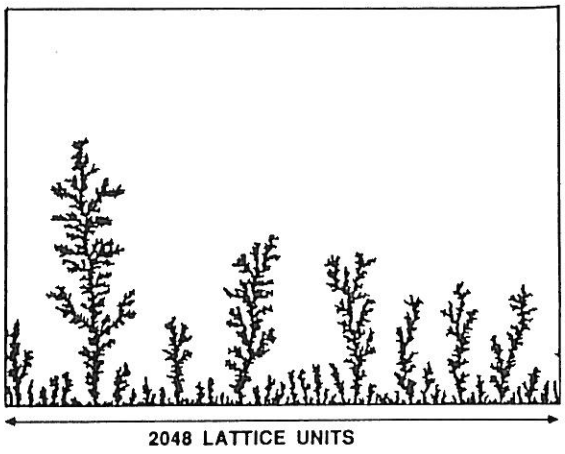

Figure 6.15. Forest of clusters grown on the square lattice along a 300 lattice unit long straight substrate. Because of screening, diffusion-limited deposition leads to a power law distribution of tree sizes (Meakin 1983b).

vant limiting case, and its investigation is expected to be helpful in understanding more complicated systems used in commercial processes. The main difference between free aggregation and deposition is in the boundary condition: In the latter case a d_s dimensional surface of nucleation sites is present instead of a single seed particle. As the simulations show (Fig. 6.15) the presence of the surface and the competition of the incoming particles result in a forest of tree-like structures. For our purposes a cluster can be defined as a collection of particles connected to the same nucleation site through nearest neighbours.

Let us first summarize the results of simulations concerning the global structure of deposits grown in two dimensions along a linear substrate of length L. The distribution of particle density is very inhomogeneous in the direction perpendicular to the substrate. This can be studied by calculating the normalized number of particles at a height h, $\rho(h) = L^{-1}\sum_x \rho(h,x)$, where $\rho(h,x) = 1$ if the lattice site at (h,x) is filled and is equal to zero otherwise. The plot of $\ln\rho(h)$ versus $\log h$ suggests that for $h \ll L$ the density $\rho(h)$ behaves as (Meakin 1983b)

$$\rho(h) \sim h^{-\alpha_\parallel} \tag{6.38}$$

with $\alpha_{||} \simeq 0.29$. Here $||$ denotes the direction parallel to the direction of growth. An effective fractal dimension can also be defined for deposits through the relation

$$N(h) \sim h^{D_s - d_s} \tag{6.39}$$

where $N(h)$ is the number of deposited particles within a distance h from the substrate. Since $N(h) \sim \int_0^h \tilde{h}^{-\alpha_{||}} \tilde{h}^{d-d_s-1} d\tilde{h}$, the above effective dimension is $D_s = d - \alpha_{||}$, in analogy with (2.18). Assuming that the correlations in the deposit decay in the same way as in a DLA cluster, we conclude that the effective dimension of deposites coincides with that of diffusion-limited aggregates ($D_s = D_{DLA}$).

The density correlations within a layer of a two-dimensional deposit provide relevant information about the internal structure of the deposit. To investigate the correlations along the lateral direction x (parallel to the deposition line) one can use the expression (Meakin *et al* 1988)

$$c_h(x) = \frac{1}{L} \sum_{x'} \rho(h, x + x')\rho(h, x'). \tag{6.40}$$

The results for the lateral correlation function are shown in Fig. 6.16a. The $c_h(x)$ curves exhibit a number of interesting features. For all h values they have a well pronounced minimum followed by a less apparent maximum. The position of the minima $x_{min}(h)$ depends on the height at which the correlation function was calculated. The corresponding log-log plot supports that the position of the minima scales with h according to an exponent $\simeq 0.8$.

One can also attempt to scale the correlation function $c_h(x)$ measured at different heights (h) onto a common curve. Fig. 6.16b shows that the correlation function can be described quite well in terms of the scaling form

$$c_h(x) \sim h^{-\alpha_{||}} f(x/h^{\delta}), \tag{6.41}$$

where the exponents $\alpha_{||}$ and δ have values of 0.275 and 0.8, respectively.

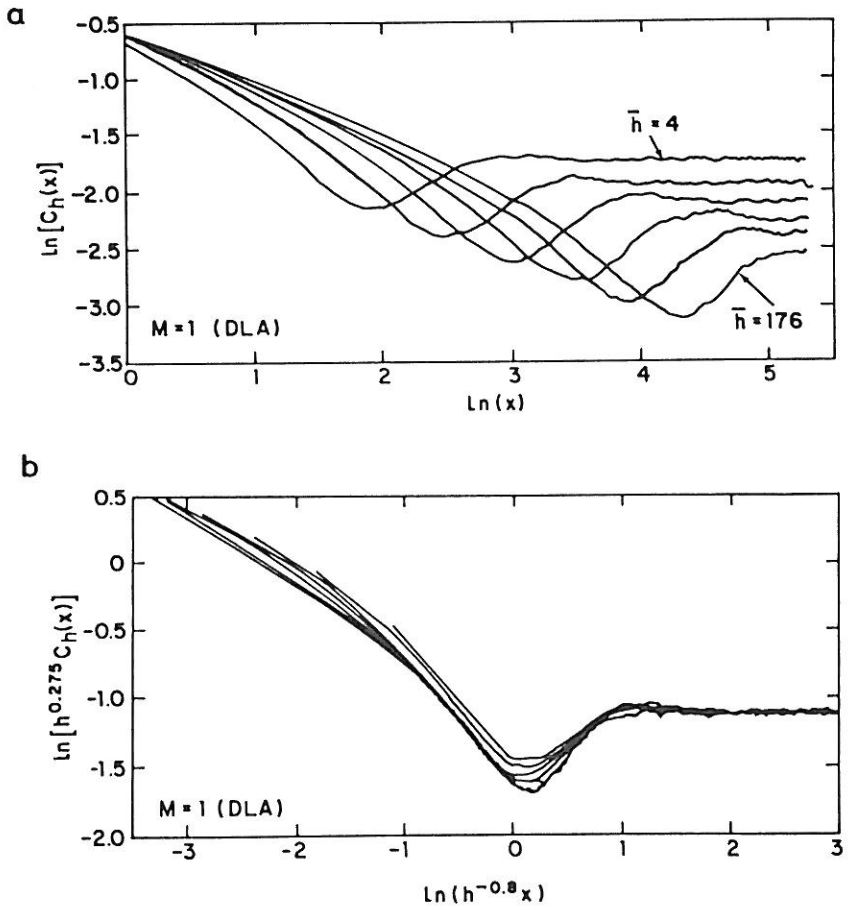

Figure 6.16. (a) Density correlations $c_h(x)$ in the lateral (x) direction within a layer of a two-dimensional deposit being at a distance h from the substrate. (b) The data for various h are shown to collapse into a single curve using the scaling form 6.41 (Meakin *et al* 1988).

Finally, the behaviour of $c_h(x)$ is nontrivial for $x \ll h$. The slope of the curve seems to approach the limiting value $\alpha_\perp \simeq 0.42$ which indicates that the decay of correlations in the lateral directon is faster than in the direction parallel to the growth, and

$$c_h(x) \sim x^{-\alpha_\perp} \qquad \text{for} \qquad x \ll 1. \tag{6.42}$$

The above results suggest that the trees are *anisotropic*. and that $\alpha_\parallel$ and $\alpha_\perp$ are close to the analogous exponents determined for the radial DLA clusters. Therefore, it is of interest to calculate the dependence of mean tree height

$$N = \sum_{s=1}^{\infty} s n_s(N) \sim \int^{\infty} s^{1-\tau} f(s^{\sigma}/N) ds$$
$$= \sigma^{-1} N^{(2-\tau)/\sigma} \int^{\infty} z^{(2-\tau-\sigma)/\sigma} f(z) dz \sim N^{(2-\tau)/\sigma} \tag{6.45}$$

which leads to the scaling law (Rácz and Vicsek 1983)

$$\tau = 2 - \sigma \tag{6.46}$$

In contrast to the cluster size distributions determined for homogeneous equilibrium systems (where $\tau > 2$), for diffusion-limited deposition the inequality $\tau < 2$ must hold in order to have a diverging sum in Eq. (6.45) if N goes to infinity. Because of $\tau < 2$ the main contribution to the sum comes from the $s \gg 1$ clusters and the use of the integral for its evaluation is justified.

Assuming that the mean cluster size

$$S = \frac{\sum_{s=1}^{\infty} s^2 n_s(N)}{\sum_{s=1}^{\infty} s n_s(N)} \tag{6.47}$$

scales with N as $S \sim N^{\gamma}$ the substitution of (6.44) into (6.47) results in $\gamma = 1/(2-\tau)$ which is again different from the expression $\gamma = (3-\tau)/\sigma$ valid for percolation systems.

An important step in completing the description of scaling in diffusion-limited deposition is finding relationships connecting the exponents D_s, $\alpha_{\parallel}$, $\alpha_{\perp}$, $\nu_{\parallel}$, $\nu_{\perp}$ characterizing the geometry of deposits and the exponents σ and τ describing the scaling behaviour of the cluster size distribution. The following argument based on scaling assumptions can be used to establish a relation connecting the two types of exponents. Since the number of clusters containing s particles decays as $n_s \sim s^{-\tau}$ one can write for the number of trees having a height larger than h_0

$$n_{h>h_0} \sim n_{s>s_0} \sim h_0^{(1-\tau)/\nu_{\parallel}}, \tag{6.48}$$

(H) and width (W) on the number of particles s in the trees. The simulations indicate that for $s \gg 1$,

$$H \sim s^{\nu_{\parallel}} \qquad \text{and} \qquad W \sim s^{\nu_{\perp}} \tag{6.43}$$

with the effective exponents $\nu_{\parallel} \simeq 0.65 \simeq 2/3$ and $\nu_{\perp} \simeq 0.56$.

An important aspect of the deposition process is that it produces a statistical *ensemble of aggregates* in a natural way. This forest of trees can be characterized by the *cluster size distribution function*, $n_s(N)$ which is the number of trees containing s particles after N particles have been deposited. Both $n_s(N)$ and N are normalized quantities and obtained from the corresponding total number of clusters and particles after a division by the area of the d_s dimensional surface onto which the deposition takes place. In large DLA clusters the density correlations decay algebraically similarly to the decay of magnetic correlations within large droplets in an equilibrium system near its critical point. Thus we expect that $n_s(N)$ exhibits a scaling behaviour analogous to that of the droplet size distribution in thermal critical phenomena (Fisher 1967) or to the cluster size distribution in percolation models (Stauffer 1985).

The related simulations (Rácz and Vicsek 1983, Meakin 1984) suggest that, indeed, the size distribution in diffusion-limited deposits can be well represented by the scaling form

$$n_s(N) \sim s^{\tau} f\left(\frac{s^{\sigma}}{N}\right), \tag{6.44}$$

where $f(x)$ is a cutoff function with $f(x) \simeq 1$ for $x \ll 1$ and $f(x) \simeq 0$ for $x \gg 1$. The above scaling behaviour is assumed to be valid for large s and N values. The expression (6.44) can be used for the derivation of a scaling law between the exponents τ and σ. The total number of particles per nucleation site, N, can be calculated through $n_s(N)$ as follows

where s_0 is the number of particles in a tree of height h_0. Using (6.48) the density of the deposit at a distance h from the substrate can be expressed as

$$\rho(h) \sim n_{h>h_0} m(h_0), \tag{6.49}$$

where

$$m(h_0) \sim \int_0^{h_0^{\nu_\perp/\nu_\parallel}} c_h(x) x^{d_s-1} dx \sim h_0^{\nu_\perp(d_s-\alpha_\perp)/\nu_\parallel} \tag{6.50}$$

is proportional to the number of particles in a layer of a tree at a distance h_0 from the substrate, and for the correlation function describing the density decay (6.42) was assumed. Substituting (6.38), (6.48) and (6.50) into (6.49) we get

$$\tau = 1 + \alpha_\parallel \nu_\parallel + (d_s - \alpha_\perp)\nu_\perp \tag{6.51}$$

which is a scaling relation among the exponents introduced earlier. For $\alpha_\parallel = \alpha_\perp = \alpha = d - D_s$ and $\nu_\parallel = \nu_\perp = 1/D_s$ the expression (6.51) leads to (Rácz and Vicsek 1983)

$$\tau = 1 + \frac{d_s}{D_s} \tag{6.52}$$

which relates the exponent describing the power law decay of the cluster size distribution to the fractal dimension for the case of deposits with isotropic scaling.

The above theoretical predictions have been tested by various approaches. The simulations of diffusion-limited deposition led to a cluster size distribution decaying as a power law for intermediate values of s and decreasing much faster for s larger than a characteristic value depending on N. According to large scale numerical experiments (Meakin 1984) the value of τ for $d_s = 1$ and $d = 2$ is $\tau \simeq 1.55$ in good agreement with both (6.51) and (6.52), since they predict $\tau \simeq 1.5$ (with $\alpha_\parallel = 0.3$, $\alpha_\perp = 0.4$, $\nu_\parallel = 2/3$ and

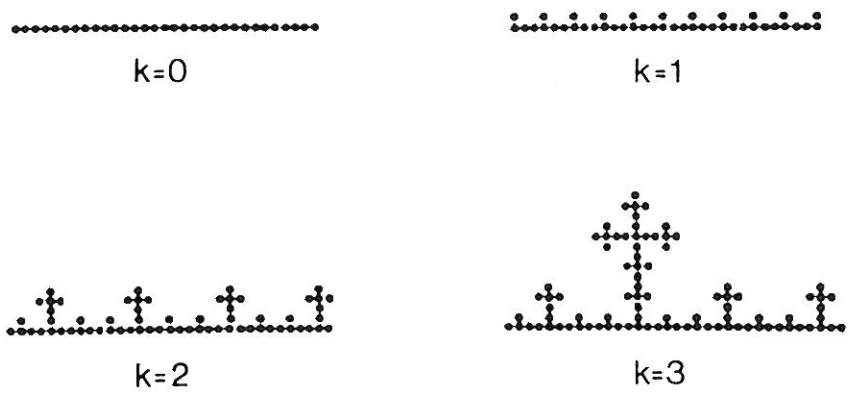

Figure 6.17. Deterministic fractal model for diffusion-limited deposition (Vicsek 1983).

$\nu_\perp = 1/2$) and $\tau \simeq 1+1/1.7 \simeq 1.59$. For $d_s = 2$ and $d = 3$ the value $\tau \simeq 1.84$ was obtained in the simulations, while (6.52) would give (with $D_s \simeq 2.5$) $\tau \simeq 1.8$.

Another possibility for checking the validity of the scaling form (6.44) and the scaling laws (6.46) and (6.52) is to calculate the corresponding quantities using a deterministic fractal model for diffusion-limited deposition (Vicsek 1983). According to this approach the deposit is generated by a recursion whose stages are demonstrated in Fig.6.17. The resulting structure has a geometry analogous to the deterministic fractal shown in Fig. 2.1a. In order to obtain the cluster size distribution, one should note that the largest clusters generated in the k-th stage of the deposition process contain $s_{max}(k) \sum_j^k 5^{j-1} = 5^k/4$ particles and the number of these clusters per nucleation site is 3^{-k}. This means that the cutoff function in (6.47) for this case is the step function $\theta(1-4s/5^k)$. Therefore, the cluster size distribution can be written in the form

$$n_s(N) \sim \frac{1}{3^l 5^l} \theta\left(1 - \frac{4s}{5^k}\right), \tag{6.53}$$

where we took into account that the normalized number of clusters of size $5^l/4$ ($l < k$) is $2/3^{l+1}$ and that these delta function-like peaks are separated

from each other by a distance proportional to 5^l. Since $s_l \sim 5^l/4$ and $N = (5/3)^k$ one recovers the scaling form (6.44) with $\tau = 1 + \ln 3/\ln 5$ and $\sigma = 1 - \ln 3/\ln 5$, so that the scaling law (6.46) is satisfied. Since $D = \ln 5/\ln 3$, the scaling relation (6.52) is also fulfilled in the deterministic model.

6.3. DIELECTRIC BREAKDOWN MODEL

This model was introduced in order to simulate a variety of dielectric breakdown phenomena which range from atmospheric lightning to electric treeing in polymers. Although the actual physical processes can be quite different in these phenomena, the global properties of the resulting discharge patterns are very similar: they have a randomly branching, open structure resembling DLA.

Before describing the model let us outline the phenomenology of the discharge process. If an insulating material is exposed to an electric field exceeding a critical value, a conducting phase is created because a large field produces mobile charge carriers. The motion of the interface is controlled by the electric field and it is more or less stochastic in time. In the dielectric breakdown model (DBM) (Niemeyer *et al* 1984) the complicated details of the physical processes occurring at the tips of the discharge pattern are ignored, and the corresponding equations are replaced by the assumptions i) $\phi = \phi_0 = 0$ in the conducting phase, where ϕ is the electric potential satisfying Laplace's equation

$$\nabla^2 \phi = 0, \tag{6.54}$$

and ii) the growth velocity is stochastically proportional to some power η of the local electric field $\vec{\mathrm{E}} = -\nabla\phi$. The apparent analogy between DLA and DBM can be understood on the level of the equations which determine the behaviour of the two models. If the exponent $\eta = 1$ the growth probability in both growth models is proportional to the local value of the gradient of a distribution satisfying (6.54), since the probability of finding a diffusing particle at a given point is also given by the Laplace equation (Witten and

Sander 1981).

The actual model is formulated on a d-dimensional hypercubic lattice, and the Laplace operator, ∇^2, is replaced with its discrete version. For example, in two dimensions (6.54) takes the form

$$\phi_{i,j} = \frac{1}{4}(\phi_{i-1,j} + \phi_{i+1,j} + \phi_{i,j-1} + \phi_{i,j+1}), \tag{6.55}$$

where $\phi_{i,j}$ is the value of ϕ in the grid site i, j. The boundary conditions are the following

$$\phi_{i,j} = 0 \qquad \text{for sites belonging to the cluster,} \tag{6.56}$$

and $\phi_{i,j} = -1$ for sites on a large circle of radius r_0 centreed at the origin. The boundary condition describing the motion of the interface is represented by an expression for the growth probability at the site i, j adjacent to the cluster

$$p_{i,j} = C\nabla\phi^{\eta}_{i,j} = -C\phi^{\eta}_{i,j}, \tag{6.57}$$

where the normalization factor is given by $1/C = \sum \phi^{\eta}_{i,j}$ with the summation running over all of the nearest neighbour sites to the cluster. It is the exponent η which is an important extra property of DBM with regard to diffusion-limited aggregation, because η turns out to be a relevant parameter from the point of view of the fractal dimension of the patterns (Niemeyer *et al* 1984). There is another slight difference in the boundary conditions. The absorbing boundary condition used in DLA corresponds to a zero potential (probability) in the sites adjacent to the aggregate (not on the cluster itself as is the case according to (6.56) for DBM).

The simulation starts with a seed particle at the origin of a lattice. The potential for each site of the lattice within a circle of radius r_0 is calculated using relaxation methods. (6.55) represents a system of linear algebraic equations (one equation per site) which can be solved by iteration. Relatively good convergency can be achieved by the Gauss-Seidel overrelaxation scheme

which on a square lattice has the form

$$\phi_{i,j}^{k+1} = \phi_{i,j}^{(k)} + \omega \left[\frac{1}{4} (\phi_{i-1,j}^{(k+1)} + \phi_{i,j-1}^{(k+1)} + \phi_{i+1,j}^{(k)} + \phi_{i,j+1}^{(k)}) - \phi_{i,j}^{(k)} \right] \qquad (6.58)$$

if one sweeps the sites in such a way that i and j increase as one goes to the next site. In (6.58) ω is the overrelaxation parameter. Finding an optimal value for ω by trial and error may speed up the convergence considerably. Next a perimeter site is chosen randomly, and a random number r drawn from a set of random numbers uniformly distributed between 0 and p_{max}, where p_{max} is the largest growth probability. If $r < p_{i,j}$, the perimeter site i,j is filled, and the whole procedure starts again by calculating the distribution ϕ in the presence of the new configuration.

This procedure for growing an N-site cluster requires much more computer time than generating a diffusion-limited aggregate of the same size since one has to solve the Laplace equation within a large region of radius r_0. Correspondingly, the data for the fractal dimension were obtained for clusters consisting of about 10000 particles. The simulations for $\eta = 1$ led to clusters with $D \simeq 1.70$ in good agreement with the expectation that DLA and DBM with $\eta = 1$ belong to the same universality class ($D_{DLA} \simeq 1.7$ in $2d$).

Varying η results in a non-trivial change of the fractal dimension (Wiesmann and Pietronero 1986), a property which makes the DBM model particularly interesting from a theoretical viewpoint (a direct connection between η and physical quantities has not been established). Table 6.3 shows the numerical estimates for D.

The mean-field type argument (Section 6.1.3.) leading to the expression (6.23) for the fractal dimension of DLA clusters can be generalized to take into account the effects of the growth exponent η. The result is given by (Matsushita et al 1986)

$$D(\eta) = \frac{d^2 + \eta(D_w - 1)}{d + \eta(D_w - 1)} \qquad (6.59)$$

which should be compared with the results given in Table 6.3. The agreement

Table 6.3. Fractal dimension for several values of the probability exponent η of the dielectric breakdown model. The data were obtained for clusters consisting of N particles and generated on d-dimensional lattices (Wiesmann and Pietronero 1986).

d	η	D	N
2	0	2.00	20000
2	0.5	1.92	30000
2	1	1.70	10000
2	2	1.43	3000
3	0	3.00	20000
3	0.5	2.78	10000
3	1	2.65	4000
3	2	2.26	1500

is good, e.g., for $d = 3$ and $\eta = 2$ expression (6.59) predicts $D = 2.2$, while the numerical value is $D \simeq 2.26$.

Finally, the distribution of the growth probabilities $p_{i,j}$ represents a fractal measure, just like in the case of DLA. The corresponding hierarchy of exponents can be determined numerically (see Fig. 6.11), leading to results being in reasonable agreement with the expectations.

6.4. OTHER NON-LOCAL PARTICLE-CLUSTER GROWTH MODELS

DLA has attracted great interest because of its obvious relevance to a large class of important physical processes. The success of diffusion-limited aggregation models has prompted a rapid increase in the number of various non-local cluster growth models leading to fractal structures. Many of these new constructions have been shown to exhibit remarkable scaling behaviour. However, none of them has such a direct relation to any significant physical phenomenon as DLA has to diffusion-limited growth. Therefore, the investigation of these models is important from a didactical point of view rather than for describing real processes.

The *screened growth* model (Rikvold 1982, Meakin *et al* 1985a) is truly non-local, since the probability of adding a particle to the cluster at site i is determined by the position of all the other particles in the aggregate. This probability for the ith perimeter site of an N particle cluster is given by

$$p_i = \frac{\prod_{j=1}^{N} e^{-Ar_{ij}^{-\lambda}}}{\sum_{k=1}^{N_s} \prod_{j=1}^{N} e^{-Ar_{kj}^{-\lambda}}} = \frac{P_i}{\sum_{k=1}^{N_s} P_k}, \tag{6.60}$$

where N_s is the total number of perimeter sites, r_{ij} is the distance of the jth particle to the ith perimeter site and A is a constant which does not affect the scaling behaviour. Because of the long-range, independent multiplicative nature of the contributions coming from the particles already belonging to the aggregate, a cluster grown according to (6.60) is a fractal. Computer simulations and theoretical considerations suggest that for this model

$$D = \lambda. \tag{6.61}$$

The following heuristic argument (Meakin *et al* 1985) supports the above relationship. Let us imagine that the cluster grows by adding sites at a rate P_i given in (6.60), so that $\sum_k P_k$ is the average number of sites created in unit time. It is possible to estimate the D-dependence of the rate P_i by changing the summation to integration when calculating the exponent describing the behaviour of P_i as a function of the distances r_{ij}

$$\sum_{j=1}^{N} r_{ij}^{-\lambda} \sim \int_a^R r^{D-1-\lambda}\, dr \sim BR^{D-\lambda}, \tag{6.62}$$

where a is a short distance cutoff length of the order of the lattice unit, B is a constant and $R \gg 1$ is the cluster radius. Supposing that $D > \lambda$ we have $P_i \sim e^{-BR^{D-\lambda}}$ and

$$\sum_{k=1}^{N_s} P_k \leq R^D e^{-BR^{D-\lambda}} \ll 1. \tag{6.63}$$

The above expression implies that the growth slows down dramatically everywhere with R becoming large. This is not expected to occur, since the formation of any branches protruding from the more compact structure can grow much faster than the other regions. On the other hand, such unstable perturbations decrease the fractal dimension D. Accordingly, a state with $D < \lambda$ has to be reached. However, it is the largest $D < \lambda$ which will be most favourable on combinatorial grounds: the number of different possible ways to obtain a given cluster shape by successive addition of sites increases with the fractal dimension of the cluster.

Studying the properties of the screened growth model requires large amounts of computer time because the growth probabilities p_i have to be updated for all of the perimeter sites after each growth event. The reward for the extra cost is a knowledge of p_i with a high accuracy, making it possible to carry out a detailed scaling analysis of the growth probability measure.

As was discussed in Section 6.1.4., if the distribution of growth probabilities can be described in terms of a fractal measure characterized by a spectrum of singularities of strength

$$\alpha = -D \ln p / \ln N, \tag{6.64}$$

then the quantity

$$f(\alpha) = D \ln[pN(p) \ln N] / \ln N \tag{6.65}$$

corresponds to the fractal dimension of the set of singular parts with strength α. Here $pN(p)d\ln p$ is the number of sites with probabilities in the range $\ln p$ to $\ln p + \ln dp$ expressed through $N(p)$ which is the number of sites with p between p and $p + dp$ divided by dp. Fig. 6.18 shows the results for $f(\alpha)$ determined for $\lambda = 1.5$ (Meakin 1987). The fact that the plots obtained for various cluster sizes N collapse onto a single curve demonstrates the existence of a unique $f(\alpha)$ spectrum.

Diffusion-limited aggregation with *disaggregation* (Botet and Jullien

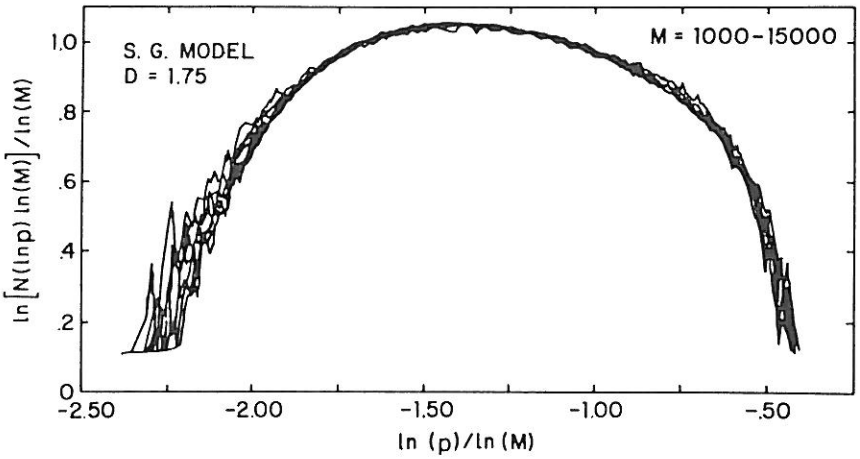

Figure 6.18. Scaling of the growth probability distribution for screened growth clusters with a fractal dimensionality of 1.75 (Meakin 1987a).

1985) is an interesting modification of the original DLA model, because during its simulation an equilibrium type regime is attained. In this lattice model a cluster is defined as a set of particles connected by filled bonds (not all of the bonds of the underlying lattice are filled). Given a cluster of N particles and the corresponding bond configuration at time $t_0 = 0$, one chooses with the same probability one of the particles which is linked to the rest of the cluster by only one bond. This particle is then allowed to diffuse away, and as in DLA it sticks to the cluster again forming a single new bond when it arrives at an adjacent site to the aggregate. At this point ($t = 1$) a new single connected particle is chosen randomly, and so on. In case the particle gets too far from the aggregate, it is eliminated and a new one is simultaneously released from a randomly selected point on a sphere centreed at the origin of the cluster and having a radius just exceeding that of the aggregate.

This model does not seem to represent any realistic physical process because the strength of a bond depends in a rather unusual way on the actual configuration. Nevertheless, it is of interest to compare the resulting structures with those generated by other aggregation or equilibrium models. Fig. 6.19 shows the process of approaching the steady-state configuration from two qualitatively different initial cluster shapes. The fractal dimension determined from the simulation of diffusion-limited aggregation with disag-

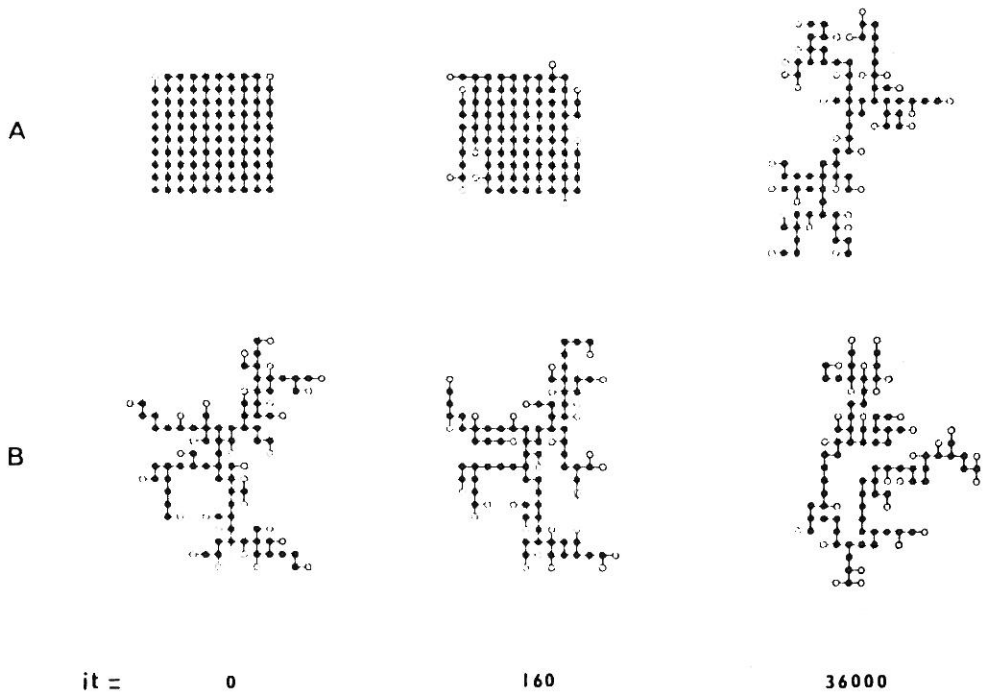

Figure 6.19. The process of aggregation with disaggregation results in qualitatively equivalent clusters even if it starts from very different initial configurations (Botet and Jullien 1985).

gregation on a square lattice is $D \simeq 1.54$, definitely smaller than the fractal dimension of DLA clusters. It is, however, very close to the fractal dimension $D \simeq 1.56$ of lattice animals representing a classical example of clusters existing in an equilibrium model (lattice animals are all the possible connected configurations of N particles each considered with the same weight). Obviously, in the present model two different configurations may have different weights. This was seen in the related simulations.

The growth probability distribution for diffusion-limited aggregation with disaggregation is expected to be uniform because of the equilibrium nature of the model. This can be checked by leaving a given configuration unchanged while releasing particles from the single connected places. Counting the number of trajectories terminating at the perimeter sites the retrapping probability distribution and the corresponding D_q spectrum can be determined from (6.30). According to the simulations (Hayakawa *et al* 1987) D_q is independent of q, as expected (see Fig. 6.11).

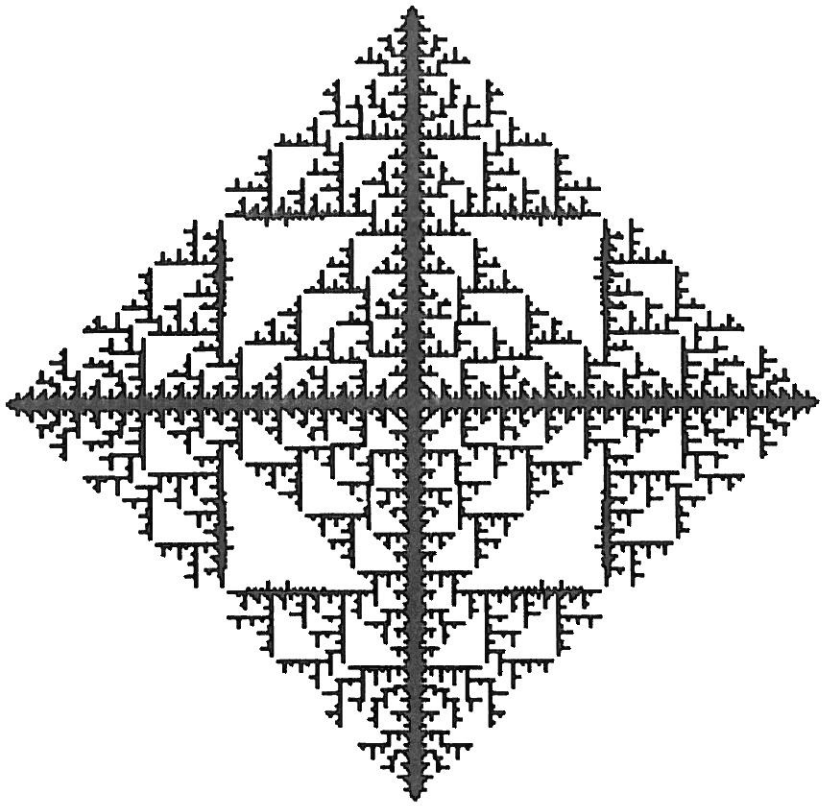

Figure 6.20. A Laplacian carpet generated on the square lattice using a deterministic version of the dielectric breakdown model. This configuration was obtained for $p = 0.45$

All models discussed in Part II so far have been stochastic concerning both the generated structures and the rules used to grow an object. This is quite understandable: the overwhelming majority of the structures existing in nature have a random geometry (it is man who prefers to produce regular shapes). Non-local growth enhances the fluctuations which leads to an increase of the already present randomness (see Chapter 9.). However, the degree of randomness can be rather different depending on the particular process considered. There are growing objects which have a simple overall shape (but still a complex surface, next Chapter), like a water droplet in the supersaturated vapor of the atmosphere. Under somewhat different circumstances, instead of a droplet a snow crystal starts growing and the resulting structure usually has a complicated regular structure.

Deterministic aggregation models lead to clusters with perfect symme-

try corresponding to the lattice on which the aggregation takes place. To obtain a noiseless structure which is grown in the presence of a diffusion field one can consider the following deterministic variation of the dielectric breakdown model. The process starts with a seed particle. The distribution of the electric potential satisfying (6.54) is calculated with the boundary condition $\phi = 0$ on the cluster and $\phi = -1$ on a circle (in $d = 2$) far from it.

From this point the two algorithms are different. In the deterministic model (Garik 1985, Family *et al* 1987) each surface site is considered for occupation simultaneously. At a given time step, all perimeter sites for which $\nabla\phi_i = \phi_i > p$ are filled, where ϕ_i denotes the potential at the ith perimeter site and $0 < p < 1$ is a fixed parameter. Next the potential distribution is calculated for the new configuration, more particles are added, and so on. Although simple, this method produces regular *Laplacian carpets* with a fractal dimension which can be tuned by changing p. Fig. 6.20 shows a typical example. Note, that while in the case of dielectric breakdown model a branch advances with a probability linearly proportional to the local gradient, in the present model this dependence is a deterministic step function.